International Pacific Research Center

April 2010 - March 2011 Report

School of Ocean and
Earth Science and Technology
University of Hawai'i at Mānoa

CONTENTS

Editor: Gisela E. Speidel, PhD
Japanese Translator: Keiko Tokinaga
Cover Photo: Gisela E. Speidel, PhD

THE INTERNATIONAL PACIFIC RESEARCH CENTER

Conceived under the "US–Japan Common Agenda for Cooperation in Global Perspective," the International Pacific Research Center (IPRC) was established in 1997 within the School of Ocean and Earth Science and Technology at the University of Hawai'i at Mānoa. The IPRC mission is "To provide an international research environment dedicated to improving mankind's understanding of the nature and predictability of climate variations and change in the Asia-Pacific region, and to developing innovative ways to utilize knowledge gained for the benefit of society." The core support for the IPRC comes from the State of Hawai'i through the University and from the principal supporting agencies: the Japan Agency for Marine-Earth Science and Technology (JAMSTEC), NASA and NOAA. Financial support for our research is also provided by other government agencies in the US and abroad. The IPRC now has an annual budget of roughly 7 million dollars.

Asia and the Pacific region are home to over half the world's people, all of whom are affected by variations in the climate system. IPRC researchers conduct modeling and diagnostic studies to document these variations and understand their causes, whether such causes are purely natural or have a human component. Through advances in basic research, the IPRC contributes to improving environmental forecasting for the Asia-Pacific region. One focus of IPRC investigations is the understanding of key phenomena rooted in the tropics, such as the El Niño-Southern Oscillation of the ocean-atmosphere system, monsoon circulations, interannual variability in the Indian Ocean, intraseasonal oscillations of the tropical atmosphere, and tropical cyclones. Other examples of important issues for IPRC study include the nature of decadal variability in the extratropical North Pacific Ocean, the dynamics of the very strong Kuroshio and Oyashio ocean currents in the western North Pacific and the role of marginal seas in the climate system. Concerns about climate change are addressed through modeling studies of past climate and through assessment of model predictions for future trends in climate.

国際太平洋研究センター

　国際太平洋研究センター（IPRC）は、「地球的展望に立った協力のための日米共通課題」のもと、1997年にハワイ大学マノア校の海洋地球科学技術学部内に設立されました。その使命は、「国際色豊かな研究環境を創り、アジア・太平洋地域の気候変動及び変化について、その性質と予測可能性に対する人類の理解を向上させ、そして得られた知見を社会に役立てるために活用する革新的な手段を生み出すこと」です。IPRCの研究費は主に、ハワイ大学を通してハワイ州から、また主要支援機関である海洋研究開発機構、NASA、NOAAから支援されています。内外のその他の政府機関からも支援を受けており、現在およそ七百万ドルの年間予算により運営しています。

　アジア・太平洋地域は世界人口の半分以上が居住する地域で、気候系の変動はこれらの人々すべてに影響を及ぼします。そのような気候変動には純粋な自然現象であるものも人類活動が関係したものもありますが、IPRCでは、それらを記述し原因を探るため、モデルによる研究や診断的研究を実施しています。このような基礎研究を進展させることでアジア・太平洋地域の環境予測の改善に大きく貢献しています。現在IPRCでは、エルニーニョ・南方振動、モンスーン循環、インド洋の経年変動、熱帯大気の季節内振動、そして熱帯低気圧といった、熱帯起源の現象に注目して研究を行っています。その他の重要な課題として、北太平洋亜熱帯域における十年規模変動の性質、西部北太平洋の強い海流である黒潮・親潮の力学、気候系での縁辺海の役割に関する研究を行っています。さらに、過去の気候のモデル研究やモデルによる将来予測の評価により、気候変化に関する様々な課題に取り組んでいます。

FOREWORD

This report summarizes the activities of the International Pacific Research Center for the period April 1, 2010–March 31, 2011. The IPRC performs research to enhance understanding of the nature and mechanisms of climate variability and change, and to improve the tools for modeling and forecasting the climate system. The IPRC now has a scientific staff of over 50 including faculty, researchers, postdoctoral fellows, and extended-term scientific visitors. IPRC faculty also supervise several graduate students in the Meteorology and Oceanography departments of the University of Hawai'i at Mānoa. In addition, via our Asia-Pacific Data Research Center (APDRC), the IPRC operates a web-based server system that makes data resources readily accessible to IPRC researchers, the international climate community, and the wider public.

Readers of this report will see the IPRC is continuing its strong programs in basic research to understand the workings of the Asia-Pacific climate system and is pursuing activities that help improve climate forecasts on seasonal to centennial timescales.

Moreover, IPRC scientists are increasingly contributing to collaborative projects on aspects of regional climate vulnerability and adaptation. Opportunities for IPRC involvement in such applied projects to support planning for sustainable communities can be expected to grow in the future.

The staff of the IPRC are grateful to our principal supporting agencies JAMSTEC, NASA and NOAA, and to the State of Hawai'i for its sponsorship of the IPRC through the University of Hawai'i. We look forward to many more years of fruitful international collaboration as we address critically important challenges in climate science.

Kevin P. Hamilton
Director

はじめに

本冊子では、国際太平洋研究センター（IPRC）における2010年4月1日から2011年3月31日までの活動概要を報告いたします。IPRCは、気候変動及び気候変化の性質とそのメカニズムに対する理解を深め、気候系のモデル化と予測に必要な道具を改良するための研究を行っています。現在、総勢50名を超える、教授陣、研究員、博士研究員、長期訪問研究員を擁し、さらに教授陣は、ハワイ大学気象学科や海洋学科の大学院生を指導しています。また、IPRCのアジア太平洋データ研究センターでは、ウェブ上にデータサーバを運用しており、IPRC内だけではなく、世界中の気候研究者に向けて、さらには広く一般の方が容易に使える形で、データを提供しています。

IPRCでは、アジア・太平洋気候系の仕組みを理解するための基礎研究を引き続き強力に推進しますと共に、数ヶ月から百年程度の時間規模での気候変動予測の改善につながる研究活動を行って参りました。

さらに、気候変動に対する地域的な脆弱性と適応の側面を取扱う共同研究に貢献する研究者も増えています。持続可能な社会の構築に役立つこのような応用研究にIPRCが貢献する機会は今後ますます増えるでしょう。

IPRCの主要支援機関である海洋研究開発機構、NASA、NOAAに対して、またハワイ大学を通して資金を提供してくださるハワイ州に対して、IPRC一同、深く感謝いたします。気候科学における喫緊の課題に取り組むことにより、今後も末永く実り多き国際的な研究協力が続くことを期待しています。
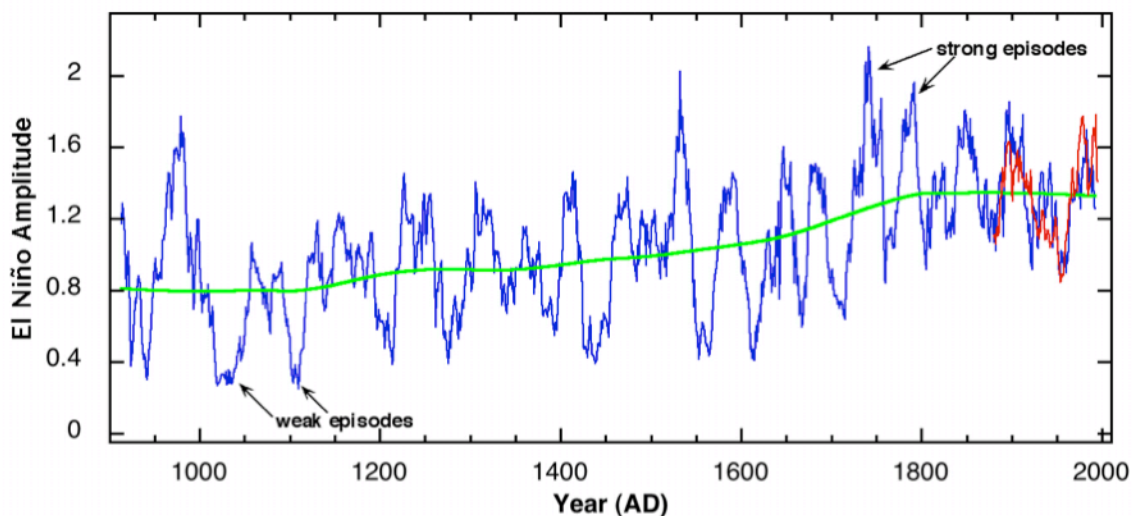
所長　ケビン P. ハミルトン

Chapter 1: LARGE-SCALE INDO-PACIFIC CLIMATE

ENSO activity during the past millennium

Annually resolved tree-ring records from the US Southwest reflect variations in the El Niño-Southern Oscillation as shown by their high correlation with a 150-year instrumental record of tropical Pacific sea surface temperature and with reconstructions from $\delta^{18}O$ isotope concentrations of live and fossil corals in the central Pacific. Analyzing such tree-ring records over the past 1,100 years reveals decades of strong El Niño events and decades of significantly reduced activity. Core samples from lake sediments in the Galapagos, northern Yucatan, and the Pacific Northwest show that the eastern–central tropical Pacific climate has warm and cool phases, each lasting from 50 to 90 years. During warm phases, El Niño and La Niña events were more intense, deviating much from the long-term average; during cool phases, they deviated little. The tree-ring data thus offer key observational benchmarks for evaluating and improving climate models and their predictions of the El Niño-Southern Oscillation under global warming.

El Niño amplitude based on North American tree rings (blue) and instrumental measurements (red). Green curve shows long-term trend in El Niño strength. Amplitudes above 1.0 indicate periods of strong El Niño activity. Superimposed on a general rising trend, cycles of strong activity occurred about every 50–90 years.

[J. Li, S.-P. Xie, E. R. Cook, G. Huang, R. D. Arrigo, F. Liu, J. Ma, and X.-T. Zheng: Interdecadal modulation of El Niño amplitude during the past millennium. *Nature Climate Change*, in press; IPRC-774]

Atmospheric teleconnections over East Asia

The interannual variability in Meiyu-Baiu precipitation induced by circulation changes was analyzed. The investigation was motivated by, the hypothesis that changes in horizontal temperature advection in the mid-troposphere adiabatically induce anomalous vertical motion and hence precipitation. The circulation anomalies were found to be related to several teleconnections, indicating remote induction effects on rainfall. In particular, studying the dynamics of the Pacific-Japan pattern it was found that this teleconnection pattern is excited by

sea surface temperature anomalies over the tropical Indian Ocean, explaining the observed lag correlation between ENSO and Meiyu-Baiu precipitation

[Y. Kosaka, S.-P. Xie, and H. Nakamura: Dynamics of interannual variability in summer precipitation over East Asia. *J. Clim.*, in press; IPRC-771]

Indian Ocean climate

Studies reported in last year's report showed how the effects of El Nino events linger as a persistent warming of the surface waters of the tropical Indian Ocean, an effect referred to as the Indian Ocean "capacitor". Further studies related to the capacitor effect and its consequences were conducted this year 1) The Indian Ocean capacitor effect strengthened in the 1970s associated with enhanced ENSO variability and enhanced response of Indian Ocean SST and tropospheric temperature. As a consequence, summer climate in the Northwest Pacific showed a strengthened correlation with ENSO six months in advance. 2) Slow modulation of Indian Ocean variability was investigated for the past 138 years (1870–2007) by the innovative use of enhanced observations along a frequent ship track from the Gulf of Aden across the North Indian Ocean and South China Sea through Malacca Strait. 3) The seasonal forecast skills of a dozen or so coupled models were evaluated for the Indo-western Pacific. They generally show skill in predicting summer atmospheric circulation anomalies over the subtropical Northwest Pacific associated with the Indian Ocean capacitor effect. 4) A new manifestation of the Indian Ocean capacitor effect was found in tropical cyclone activity in the Northwest Pacific; the tropical cyclone count does not differ much in El Niño and La Niña phases but decreases substantially in the summer following El Niño. The typhoon season of 2010 is a good example, especially the first half. 5) Finally, in an investigation of the semiannual cycle in zonal wind over the equatorial Indian Ocean, a momentum budget analysis showed that momentum advection generated by the cross-equatorial monsoon circulation is important for the semiannual zonal-wind cycle in the equatorial Indian Ocean.

[S.-P. Xie, Y. Du, G. Huang, X.-T. Zheng, H. Tokinaga, K. Hu, Q. Liu, 2010: Decadal Shift in El Niño Influences on Indo–Western Pacific and East Asian Climate in the 1970s. *J. Clim.*, **23**, 3352–3368. doi: 10.1175/2010JCLI3429.1; IPRC-669; Y. Du, L. Yang, and S.-P. Xie, 2011: Tropical Indian Ocean influence on Northwest Pacific tropical cyclones in summer following strong El Nino. *J. Clim.*, **24**, 315-32; IPRC-730; J.S. Chowdary, S.-P. Xie, J.-Y. Lee, Y. Kosaka, and B. Wang, 2010: Predictability of summer Northwest Pacific climate in 11 coupled model hindcasts: Local and remote forcing. *J. Geophys. Res.-Atmos.*, **115**, D22121, doi:10.1029/2010JD014595. IPRC-716; T. Ogata and S.P. Xie].

Volcanic forcing of the tropical Pacific

The response of the El Niño-Southern Oscillation (ENSO) to massive volcanic eruptions was studied in a suite of Coupled General Circulation Model (CGCM) simulations utilizing the Community Climate System Model, version 3 (CCSM3). We found that the radiative forcing due to volcanic aerosols injected into the stratosphere induces a climate response that projects onto the ENSO mode and initially creates a La Niña event, which peaks around the time the volcanic forcing peaks. The change in the wind stress curl accompanying this volcanically-forced cooling of the equatorial region acts to recharge the equatorial region heat. For weaker volcanic eruptions, this recharging results in an El Niño event about 2 seasons after the peak of the

volcanic forcing. The results of our CCSM3 volcanic forcing experiments lead us to propose that the initial tropical Pacific Ocean response to volcanic forcing is determined by four different mechanisms. One mechanism is the dynamical thermostat (the mean upwelling of anomalous water temperature); the other processes are related to the zonal equatorial gradients of the mean cloud albedo, radiative response, and mixed-layer depth. We found that in CCSM3 the zonal gradient set by both mixed-layer depth and radiative response terms oppose the zonal sea surface temperature anomaly (SSTA) gradient produced by the dynamical thermostat and initially dominate the mixed-layer zonal equatorial heat budget response. When we applied this information to a simple volcanically forced mixed-layer equation using observed estimates of the spatially varying variables, we found again that the mixed-layer depth and radiative response terms oppose and dominate the zonal SSTA gradient produced by the dynamical thermostat. This implies that the observed initial response to volcanic forcing should be La Niña-like, whereas the subsequent stages of the equatorial response are dominated by the recharging of the equatorial thermocline and the increased chance to generate an El Niño event.

[S.A. McGregor, A. Timmermann: The response of ENSO to explosive volcanic eruptions, *J. Clim.*, in press; IPRC-740]

ENSO phase-locking to the annual cycle

The El Niño-Southern Oscillation (ENSO) is the largest global climate signal on the interannual timescale. ENSO events occur irregularly, yet individual events follow a similar pattern of developing during boreal summer/fall and peaking during boreal winter. This characteristic of ENSO is often referred to in the climate literature as the "phase locking" of ENSO with the annual cycle. However, no evidence of phase interaction between ENSO and the annual cycle has thus far been presented. In this study, the analysis of complex EOFs of sea surface temperature observations together with the phase-time series of ENSO and the annual cycle provide the first evidence of partial-phase synchronization between ENSO and the annual cycle.

[K. Stein, A. Timmermann, N. Schneider, Phase synchronization of ENSO and the annual cycle, submitted to *Phys. Rev. Lett.*]

The effect of the SPCZ on ENSO termination

The westerly wind response to an El Niño event shifts southward during boreal winter and early spring such that the maximum zonal wind is centered about 5–7 degrees south of the equator. The resulting meridional asymmetry, along with a related seasonal weakening of wind anomalies on the equator, is a key element in the termination of strong El Niño events. Simulation with an intermediate complexity 2.5-layer atmospheric model demonstrated that these features result from a weakening of the climatological wind speeds south of the equator associated with the seasonal intensification of the South Pacific Convergence Zone (SPCZ) and hence a reduced surface damping of the combined boundary-layer/lower-tropospheric wind response to El Niño. Furthermore, this southward wind generates a meridionally asymmetric discharge of heat away from the equator.

[McGregor, S, A. Timmermann, N, Schneider: On the meridional asymmetry of ENSO, in preparation]

Tropical Atlantic climate

Observational analysis and an ocean GCM simulation show that the Benguela Niño, which takes place on the west coast of southern Africa and peaks in boreal spring, is closely related to the subsequent development of its cousin on the equator, the Atlantic Niño: both are related to variability in the subtropical high over the South Atlantic. The origin of equatorial Atlantic biases in coupled models was investigated with a series of experiments based on a GFDL coupled model. The experiments confirm the impact of wind biases in boreal spring on the cold tongue biases.

[J.F. Lubbecke, C.W. Boning, N.S. Keenlyside and S.-P. Xie, 2010: On the connection between Benguela and equatorial Atlantic Niños and the role of the South Atlantic Anticyclone. *J. Geophys. Res.-Oceans,* **115***,* C09015, doi:10.1029/2009JC005964; IPRC 787; I. Richter, S.-P. Xie, A.T. Wittenberg, Y. Masumoto: Tropical Atlantic biases and their relation to surface wind stress and terrestrial precipitation. *Clim. Dym.*, in press; IPRC-765]

Global warming dynamics

A number of projects were conducted that focused on the ocean's role in global warming, specifically on regional patterns in both observed 20th century and projected 21st century climate change .1) In contrast to climate model simulations and moist adiabatic lapse rate adjustment (MALR) theory, some observations show that the tropical troposphere may have become more unstable over the past decades, implying a nearly constant sea surface temperature (SST) threshold for convection and an increased convection rate. A 30-year time series, however, shows that both annual mean tropical SST and two different estimates of SST threshold for convection have risen together by about 0.1°C per decade. Both estimates show a high correspondence (r>0.88) between tropical mean SST and threshold on interannual and longer timescales, suggesting that recent tropospheric trends are consistent with MALR adjustment. Analysis of 10 CMIP3 global climate-model simulations into the 21st century suggests that SST convection threshold will rise in tandem with tropical mean SST as a consequence of moist adiabatic adjustment. Thus, no substantial increase is expected in the fraction of convectively active tropical ocean areas.

To investigate whether sea surface wind shows a spurious rising trend due to the increase in anemometer height over the last 50 years, a bias-corrected marine surface wind product was constructed with the innovative use of wind-wave heights that have been logged by ships for years. Using this surface wind product, robust patterns of tropical Atlantic climate change over the last six decades were detected. The changes are characterized by weakened spatio-temporal variations in equatorial climate indicators.

A regional ocean-atmosphere coupled model was used to downscale an A1B climate projection from a global climate model, in what may be the first study of its. The downscaling simulated realistic tropical instability waves (TIWs), permitting an assessment of their response and impact in a changing climate. TIWs increased in strength, impacting equatorial dynamics and suggesting a need for their sustained monitoring with spatially denser observational arrays in the equatorial oceans than at present.

[N.C. Johnson and S.-P. Xie, 2010: Changes in the sea surface temperature threshold for tropical convection *Nature Geosci.*, **3**, 842-845. IPRC-751; H. Tokinaga, and S.-P. Xie, 2011: Wave and Anemometer-based Sea-surface Wind (WASWind) for climate change analysis. *J. Clim.*, **24**, 267-

285. IPRC-718; H. Tokinaga, and S.-P. Xie, 2011: Weakening of the equatorial Atlantic cold tongue over the past six decades. *Nature Geosci.*, **4**, 222-226, doi:10.1038/ngeo1078. IPRC-753:H. Seo and S.-P. Xie, 2011: Response and impact of equatorial ocean dynamics and tropical instability waves in the tropical Atlantic under global warming: A regional coupled downscaling study. *J. Geophys. Res.-Oceans*, **116**, C03026, doi:10.1029/2010JC006670. IPRC-788]

Changes in western boundary currents and ocean warming trends

The subtropical western boundary currents carry warm tropical water to the midlatitudes, venting large amount of heat and moisture to the atmosphere along their path and thereby may profoundly affect midlatitude storms, the jet stream and also carbon uptake. Based on different reconstructed sea surface temperature datasets and newly developed century-long ocean and atmosphere reanalysis products, we found that the post-1900 ocean surface warming rate over the path of these currents is higher by a factor of 2 to 3 than the global mean ocean surface warming. These oceanic "hotspots" reflect a synchronous poleward shift and intensification of global subtropical western boundary currents, powered by a systematic change in winds in both hemispheres. The long-term oceanic and atmospheric circulation trends responsible for the accelerated warming in the paths of the western boundary currents are consistent with the results of greenhouse warming climate-model projections for the 21st century. The accelerated warming may reduce the capacity of the ocean to absorb the anthropogenic carbon dioxide over these regions.

[L. Wu, W. Cai, A. Timmermann et al.: Oceanic hotspots of global warming, *Geophys. Res. Lett*., submitted].

Dynamical effects of mode water

The ventilation of low potential-vorticity (PV) mode water occurs in the eastward subtropical countercurrent (STCC) in the North Pacific. The dynamical connection between mode water and STCC was the topic of a symposium at the 2010 Spring Meeting of the Oceanographic Society of Japan and the compilation of a special section on mode waters in *J. Oceanography* (guest editors, A. Kubokawa, S.-P. Xie, and F. Kobashi), due for publication in late 2011. A recent analysis of a long integration with the GFDL coupled model shows that the variability in mode-water ventilation causes changes in the STCC, forming a mode of decadal variability in the central subtropical gyre. The North Pacific response to global warming projects strongly onto this decadal mode, forming northeast-slanted bands of circulation and SST changes.

[S.-P. Xie, L.-X. Xu, Q. Liu, and F. Kobashi, 2011: Dynamical role of mode-water ventilation in decadal variability in the central subtropical gyre of the North Pacific. *J. Climate*, **24**, 1212-1225; IPRC-728]

Extratropical air-sea interaction

During a workshop with researchers of the Japanese Hotspot project at the IPRC in December 2010, further collaborations in the area of extratropical air-sea interaction were discussed. In a remarkable study, a low-pressure wedge had been detected at the sea surface in the climatology from ship reports along the Kuroshio south of Japan and its eastward extension. The wedge is caused by a hydrostatic response to intense surface heat flux and enhanced vertical mixing of momentum.

[Y. Tanimoto, T. Kajitani, H. Okajima, and S.-P. Xie, 2010: A peculiar feature of the seasonal migration of the South American rain band. *J. Meteor. Soc. Japan*, **88**, 79-90; IPRC-655]

The atmospheric response to the spring Kuroshio front over the East China Sea was investigated using a suite of high-resolution satellite data and a regional atmospheric model. The atmospheric response appears to extend beyond the marine atmospheric boundary layer, with frequent cumulus convection. In spring, QuikSCAT wind speed shows a clear effect of sea surface temperature (SST), with high (low) wind speed observed over the warm (cold) tongue. This in-phase relationship between SST and surface wind speed is indicative of SST influence on the atmosphere. Wind convergence is found on the warmer flank of the Kuroshio front, accompanied by a narrow rainband. The analysis of satellite-borne radar measurements indicates that deep convection appears over the Kuroshio warm tongue in the spring season, with enhanced convective precipitation, frequent occurrence of cumulus convection, and increased precipitation (cloud tops) in altitude. This deep convection along the Kuroshio warm tongue is also seen in the increased lightning flash rate observed by satellite and in the atmospheric heating estimates by a Japanese reanalysis. The Weather Research and Forecasting (WRF) model was used to investigate the precipitation response to the spring Kuroshio SST front over the East China Sea. Consistent with satellite observations, the model, forced by observed SST (CTL), simulates a narrow band of precipitation, high wind speed, and surface wind convergence that closely follows the Kuroshio warm current. This narrow rainband completely disappears in the model when the SST front is removed by horizontally smoothed SST. The results show that convective precipitation is sensitive to the Kuroshio SST front. A case study of an eastward-moving extratropical cyclone indicates that convective precipitation increases in intensity and duration in the CTL run compared to the smoothed SST run. Local intensification of upward sensible and latent heat fluxes and convective instability in the lower atmosphere anchor the narrow band of convective precipitation that closely follows the Kuroshio Current.

[H.-M. Xu, S.-P. Xie, and Y. Wang: Deep atmospheric response to the spring Kuroshio Current over the East China Sea. *J. Clim.*, in press, IPRC-785]

The dynamics of the Leeuwin Current and shallow eastward flow in the South Indian Ocean

Observations show that there is a shallow, broad eastward flow in the subtropical gyre of the South Indian Ocean. This is a notable phenomenon as the current is against the expected Sverdrup flow. This flow bends poleward at the west coast of Australia to form (or join) the Leeuwin Current (LC), which flows against the prevailing, equatorward winds. An inviscid 1.5-layer model was applied to study this current. This model allows the upper-layer density to vary in horizontal directions letting the upper layer "ground" and the lower layer vanish. The model was driven solely by a prescribed, meridional density gradient, which tends to drive an eastward flow. When the upper layer grounds on the shelf, the onshore flow bends poleward, forming the model's LC.

[R. Furue, J.P. McCreary, and J. Benthuysen (CSIRO/Univ. of Tasmania)]

Chapter 2: REGIONAL AND SMALL SCALE CLIMATE PROCESSES AND PHENOMENA

Modeling the seasonal variation of marine boundary layer clouds over the eastern Pacific with the IPRC regional climate model (iRAM)

Marine boundary layer (MBL) clouds off the west coasts of the continents have a great impact on climate because of their significant effect on the global radiation budget. Understanding relevant mechanisms responsible for the formation of these clouds and their observed interannual variability is therefore crucial for climate research. Spectral analysis of MBL cloud time-series reveals that most of the variability occurs on seasonal to interannual timescales. The seasonal cycle of MBL clouds over the eastern Pacific was studied with the IPRC Regional Atmospheric Model (iRAM). The results show that the model is capable of simulating not only the overall seasonal cycle but also the spatial distribution, cloud regime transition, and vertical structure of MBL clouds over the eastern Pacific. Although the modeled MBL cloud layer is generally too high in altitude over the open ocean compared with available satellite observations, the model simulated well the westward deepening and decoupling of the MBL, the rise in the cloud base and top of the low-cloud decks off the Peruvian and Californian coasts, and the cloud regime transition from stratocumulus near the coast to trade cumulus farther to the west in both the Southeast and Northeast Pacific. In both observations and the model simulation, surface latent heat flux is large and the cloud base is elevated during the season with small low-level cloudiness. This coincides with weak sub-cloud layer mixing and strong entrainment at the cloud top, characterized by high degree of MBL decoupling, whereas the opposite situation is true for the season with large low-level cloudiness. This seasonal cycle in low-level cloud properties resembles the downstream stratocumulus-to-cumulus transition of marine low-clouds and can be explained by the "deepening-decoupling" mechanism previously proposed. The seasonal variations of low-level clouds off the Peruvian coast are mainly caused by large seasonal variability in sea surface temperature (SST), while those off the Californian coast are largely attributed to the seasonal cycle in lower-tropospheric temperature.

[L. Wang, Y. Wang, A. Lauer, and S.-P. Xie,: Simulation of seasonal variation of marine boundary layer clouds over the eastern Pacific with a regional climate model. *J. Clim.,* in press; IPRC-775]

Improved representation of boundary layer clouds over the Southeast Pacific in WRF-ARW using a modified Tiedtke cumulus parameterization scheme

A modified Tiedtke cumulus parameterization (CP) scheme used in the IPRC regional climate model (iRAM) has been implemented into the Advanced Research Weather and Research Forecasting (WRF–ARW) model to improve the representation of marine boundary layer (MBL) clouds over the Southeast Pacific (SEP). A simulation for October 2006 was performed using the National Center for Environmental Predictions (NCEP) final analysis (FNL) as both the initial and lateral boundary conditions and the observed sea surface temperature (SST). The model simulation was compared with satellite observations and with results from an intense ship-based campaign of balloon soundings during 16–20 Oct 2006 at 20S, 85W.

The model with the modified Tiedtke scheme successfully captured the main features of the MBL structure and low clouds over the SEP, including the geographical distribution of MBL

clouds, the cloud regime transition, and the vertical structure of the MBL. The model simulation was repeated with the various CP schemes currently provided as standard options in WRF–ARW. The simulations with the other CP schemes failed to reproduce the geographical distribution of cloud fraction and the observed cloud-regime transition, and displayed a MBL too shallow compared to observations. The improved simulation with the modified Tiedtke scheme can be attributed to a more active parameterized shallow convection with the modified Tiedtke scheme than with the other CP schemes tested. The greater shallow convection played a critical role in lifting the inversion base and the low cloud layer

[C.-X. Zhang, Y. Wang, and K. Hamilton: Improved representation of boundary layer clouds over the Southeast Pacific in WRF–ARW using a modified Tiedtke cumulus parameterization scheme. *Mon. Wea. Rev.*, in press, IPRC-778]

Multiscale interactions in the lifecycle of a tropical cyclone simulated in NICAM

The global cloud-system-resolving model NICAM successfully simulated the lifecycle of Tropical Storm Isobel that formed over the Timor Sea in the austral summer 2006. Isobel's lifecycle was found to be largely controlled by a Madden-Julian Oscillation (MJO) event and associated westerly wind burst (WWB). The large-scale, low-level convergence and high convective available potential energy (CAPE) downwind of the WWB center provided a favorable region for cyclogenesis and intensification, whereas the strong large-scale stretching deformation field upwind of the WWB center may have weakened the storm by exciting wavenumber-two asymmetries in the eyewall, leading to the eyewall breakdown. Five stages were identified in the lifecycle of the simulated Isobel, namely, the initial eddy, intensifying, temporary weakening, re-intensifying, and decaying stages. The initial eddy stage consisted of small-/meso-scale convective cyclonic vortices that developed in the zonally-elongated rainband organized in the pre-conditioned environment and characterized by the WWB over the Java Sea associated with the onset of an MJO event over the East Indian Ocean. As the MJO propagated eastward and the cyclonic eddies moved southward into an environment with weak vertical shear and strong low-level cyclonic vorticity, a typical tropical cyclone structure developed over the Java Sea, which had its real-life counterpart in the genesis of Isobel. The modeled Isobel experienced an eyewall breakdown and a temporary weakening when it was upwind of the WWB center as the MJO propagated southeastward; it reintensified as its eyewall reformed as a result of the axisymmetrization of an inward spiraling outer rainband that originally formed downwind of the WWB center. Finally Isobel decayed as it approached the northwest coast of Australia.

The analysis for mesoscale and storm-scale processes showed that in the pre-conditioned favorable environment over the Java Sea, mesoscale convective vortices (model MCVs) developed in the mesoscale convective systems (MCSs), and convective towers with cyclonic potential vorticity (PV) anomalies appeared throughout the troposphere (model VHTs) in the model MCVs. Multiple model VHTs strengthened cyclonic PV in the interior of the model MCV and led to the formation of an upright monolithic PV core at the center of the concentric MCV (primary vortex enhancement). As the monolithic PV core with a warm core developed near the circulation center, cyclonic PV intensified and spread horizontally through the system scale intensification (SSI) process (the secondary vortex enhancement), leading to the genesis of Isobel over the Timer Sea. When the eyewall reformed as a result of the axisymmetrization of an inward propagating outer spiral rainband, the SSI process became effective again, leading to the re-intensification of Isobel. Therefore, the large-scale environmental flow provided the precondition

for the genesis of Isobel and triggered the subsequent storm-scale structure change. The mesoscale and the system-scale processes, such as the evolution of MCVs and merging VHTs, were responsible for the genesis, while the eyewall processes were critical to the storm intensity change through the SSI process.

[H. Fudeyasu, Y. Wang, M. Satoh, T. Nasuno, H. Miura, and W. Yanase, 2010: Multi-scale interactions in the lifecycle of a tropical cyclone simulated in a global cloud-system resolving model. Part I: Large- and storm-scale evolutions. *Mon. Wea. Rev*., **138**, 4285-4304, IPRC-713; H. Fudeyasu, Y. Wang, M. Satoh, T. Nasuno, H. Miura, and W. Yanase, 2010: Multiscale interactions in the lifecycle of a tropical cyclone simulated in a global cloud-system resolving model. Part II: Mesoscale and storm-scale processes. *Mon. Wea. Rev*., **138**, 4305-4327, IPRC-714]

Balanced contribution to the outer core spin-up of a simulated tropical cyclone

The primary circulation of a strong tropical cyclone is a warm-core, quasi-axisymmetric vortex in gradient-wind and hydrostatic balance. As the cyclone evolves slowly, its primary circulation remains in gradient-wind and hydrostatic balance, while a secondary circulation (radial and vertical circulation) develops as a result of both diabatic heating and momentum forcing, including surface friction. The secondary circulation transports high absolute angular momentum inward to spin up the tropical cyclone primary circulation. This spin-up process can be well described by the Sawyer-Eliassen equation.

The balanced contribution to the intensification of a tropical cyclone simulated in the three-dimensional, nonhydrostatic, full-physics model TCM4 (iCRM), in particular to the spin-up of the outer core circulation, was investigated by solving the Sawyer-Eliassen equation and by computing terms in the azimuthal-mean tangential wind equation. Results demonstrate that the azimuthal-mean secondary circulation (radial and vertical circulation) and the spin-up of the mid-tropospheric outer core circulation in the simulated tropical cyclone are well captured by balance dynamics. The mid-tropospheric inflow develops in response to diabatic heating in mid-upper tropospheric stratiform (anvil) clouds in active spiral rainbands outside the eyewall and transports absolute angular momentum inward to spin up the outer core circulation. Although the azimuthal-mean diabatic heating rate is highest in the eyewall, its contribution to radial winds and thus the spin-up of the outer core circulation in the mid-troposphere is rather small. The result thus suggests that diabatic heating in spiral rainbands is the key to the continued growth of the storm scale circulation.

[H. Fudeyasu, and Y. Wang, 2011: Balanced contribution to the intensification of a tropical cyclone simulated in TCM4: Outer core spin-up process. *J. Atmos. Sci*. in press, IPRC-741]

Impact of ENSO and East Indian Ocean SSTA on the interannual variability of Northwest Pacific tropical cyclone frequency

Earlier studies have examined the effects of El Niño on the seasonal tropical cyclone (TC) climatology. Specifically when comparing El Niño to La Niña years, the mean location of TC genesis over the WNP is displaced eastward and typhoons tend to be more intense and long-lived However, the total annual number of TCs over the WNP is not significantly correlated with the ENSO index, suggesting that other factors may determine the annual number of TCs.

An observational study showed that both ENSO and boreal summer sea surface temperature anomaly (SSTA) in the East Indian Ocean (EIO) are related to the annual TC frequency over the WNP, but their effects are very different. ENSO modulates the large-scale atmospheric circulation and barotropic energy conversion over the WNP, contributing to changes in both the TC genesis location and the frequency of intense TCs. The EIO SSTA affects significantly both the western Pacific summer monsoon and the equatorial Kelvin wave activity over the western Pacific, thereby impacting TC genesis over the entire WNP formation region and largely determining the total number of TCs. In general the warm (cold) EIO SSTA suppresses (promotes) the TC genesis over the WNP.

In another study, the impact of SSTA in the EIO on the TC frequency over the western North Pacific (WNP) and the physical mechanisms were examined using the IPRC regional atmospheric model (iRAM) driven by reanalysis data and observed SSTs. The model reproduces realistic climatic features of the WNP TC activity, including the observed statistical (negatively correlated) relationship between the WNP TC frequency and the EIO SSTA. The experiments with artificially imposed SSTA in the EIO in the year 2004 and with normal EIO SST and WNP TC activity confirm that the EIO SSTA does affect the TC genesis frequency in the entire genesis region over the WNP by significantly modulating both the western Pacific summer monsoon and the equatorial Kelvin wave activity over the western Pacific, two major large-scale dynamical controls of TC genesis over the WNP. Additional sensitivity experiments were performed for two extreme years: one (1994) with the highest and one (1998) with the lowest TC annual frequencies during the studied period. Removing the EIO SSTAs in the two extreme years, the TC frequency in 1998 is close to the climatological mean, but the number in 1994 is still above average. The model results suggest that the warm EIO might be a major factor contributing to the unusually few TCs formed over the WNP in 1998, but the cold EIO seemed to contribute little to the excessive WNP TCs in 1994.

[R.-F. Zhan, Y. Wang, and X.-T. Lei, 2011: Contributions of ENSO and East Indian Ocean SSTA to the interannual variability of Northwest Pacific tropical cyclone frequency. *J. Clim.*, **24**, 509-521; IPRC-721; R.F. Zhan, Y. Wang, and C.-C. Wu: Impact of SSTA in East Indian Ocean on the frequency of Northwest Pacific tropical cyclones: A regional atmospheric model study, submitted to *J. Clim.*]

Formation and quasi-periodic behavior of outer spiral rainbands in a numerically simulated tropical cyclone

The formation and quasi-periodic behavior of outer spiral rainbands were analyzed in a tropical cyclone simulated in the IPRC cloud-resolving tropical cyclone model TCM4. The outer spiral rainbands in the simulation were initiated near the 60-km radius, or roughly about three times the radius of maximum wind (RMW). After initiation, they generally propagated radially outward with a mean speed of ~5 m s^{-1}. They were reinitiated quasi-periodically with a period between 22h and 26h in the simulation. While the inner spiral rainbands, which form within a radius of about three times the RMW, are characterized by the convectively coupled vortex Rossby waves (VRWs), the formation of rainbands beyond this radius is much more complicated. The outer spiral rainbands were triggered by the inner-rainband remnants immediately outside the rapid filamentation zone and local inertial instability in the upper troposphere. The preferred radial location of initiation of outer spiral rainbands is understood as a balance between the suppression

of deep convection by rapid filamentation and the favorable dynamical and thermodynamic conditions for initiation of deep convection.

The quasi-periodic occurrence of outer spiral rainbands was found to be associated with the boundary-layer recovery from the effect of convective downdrafts and the consumption of convective available potential energy (CAPE) by convection in the previous outer spiral rainbands. Specifically, once convection is initiated and organized in the form of outer spiral rainbands, it will produce strong downdrafts and consume CAPE, weakening convection near its initiation location. As the rainband propagates outward further, the boundary layer air near the original location of convection initiation takes about 10 h to recover by extracting energy from the underlying ocean. Convection and new outer spiral rainbands will then be initiated near a radius of about three times the RMW, followed by a similar outward propagation and the subsequent boundary layer recovery, leading to a quasi-periodic occurrence of outer spiral rainbands. In response to the quasi-periodic appearance of outer spiral rainbands, the storm intensity shows a similar quasi-periodic oscillation with intensity or intensification rate starting to decrease after about 4 h of the initiation of an outer spiral rainband. The results provide an alternative explanation or one of the mechanisms responsible for the quasi-periodic (quasi-diurnal) variation in the intensity and in the area of outflow-layer cloud canopy of observed tropical cyclones.

[Q.-Q. Li, and Y. Wang: Formation and quasi-periodic behavior of outer spiral rainbands in a numerically simulated tropical cyclone. submitted to *J. Atmos. Sci.*]

On sea surface roughness parameterization and its effect on tropical cyclone structure and intensity

A new parameterization scheme of sea surface momentum roughness length for all wind regimes, including high winds under tropical cyclone conditions, was constructed based on measurements from Global Positioning System (GPS) dropsondes. The scheme reproduces the observed transition regime, namely, the drag coefficient increases with increasing wind speed up to 40 m/s and then decreases with further increase in wind speed. The effect of this parameterization on the structure and intensity of tropical cyclones was evaluated using the IPRC cloud-resolving tropical cyclone model TCM4. The results show that the final intensity has increased by 10.5% (8.9%) in the maximum surface wind speed and by 8.1 hPa (5.9 hPa) in the minimum sea surface pressure drop with (without) dissipative heating. This intensity increase was found to be mainly due to the reduced frictional dissipation in the surface layer and to have little to do with either the surface enthalpy flux or latent heat release in eyewall convection. The effect of the new parameterization on storm structure was insignificant and occurred only in the inner core region with increase in tangential winds in the eyewall and increase in temperature anomalies in the eye. This is because the difference in drag coefficient appears only in a small area under the eyewall.

[Z.-H. Zeng, Y. Wang, Y.-H. Duan, L.-S. Chen, and Zhiqiu Gao, 2010: On sea surface roughness parameterization and its effect on tropical cyclone structure and intensity. *Adv. Atmos. Sci.*, **27**, 335-355; IPRC-629]

Impacts of secondary eyewall heating on tropical cyclone intensity-change

Intense tropical cyclones (TCs) commonly involve formation of a secondary eyewall during which TC intensity usually, but not necessarily, decreases significantly. Some TCs, however, may intensify during secondary-eyewall formation. To identify factors pertinent to intensity changes associated with eyewall replacement we compared concentric eyewall structures in the TCs with and without weakening in the Tropical Rainfall Measuring Mission (TRMM) 2A12 and 2A25 data. It was found that *the secondary eyewalls with a stratiform-type heating profile weaken markedly, while those with a convective-type heating profile weaken insignificantly or even intensify*. This observed feature is supported by a set of sensitivity numerical experiments performed with the Weather Research and Forecasting Model. Stronger convection releases more latent heat in the outer eyewall and moat area and thereby can sustain storm intensity. In contrast prevailing stratiform precipitation in the outer eyewall and moat area induces persistent downdrafts, which reduce the equivalent potential temperature of the boundary inflow to the inner eyewall and thus leads to large intensity fluctuations. Comparison of the observations and numerical model results reveals that the model tends to overproduce convective precipitation in the outer eyewall and moat area. Therefore, the model likely underestimates the storm intensity-changes associated with eyewall replacement.
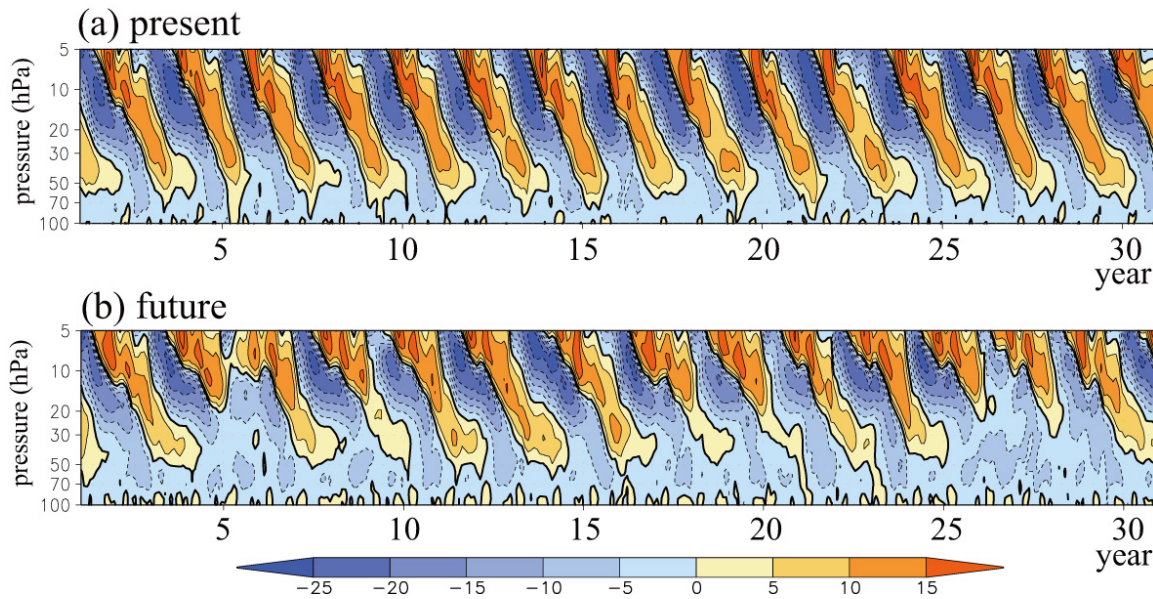
[X. Zhou, B. Wang, X. Ge, and T. Li : Impacts of Secondary Eyewall Heating on Tropical Cyclone Intensity Change, *J. Atmos. Sci.*, in press; IPRC-735]

Gravity wave forcing of the quasibiennial oscillation

The quasibiennial oscillation (QBO) of the mean wind in the tropical stratosphere is thought to be largely forced by the interaction of the mean flow with vertically propagating gravity waves of relatively small scale. The QBO represents a particularly dramatic example of strong interactions between mesocale/submesoscale phenomena with the global scale circulation. Typically global general circulation models (GCMs) fail to simulate any mean flow variation like the QBO in the stratosphere, unless a parameterization of the effects of vertically-propagating non-stationary gravity waves is included. At present such parameterizations have to be adjusted in somewhat arbitrary ways to produce a realistic QBO simulation. This approach makes projections of the response of the stratospheric circulation to climate perturbations, such as increasing greenhouse gas concentrations, very problematic. In the present work, the performance of a high vertical and horizontal resolution version of the MIROC atmospheric GCM without a parameterization of non-stationary waves, was evaluated. The model was able to simulate an equatorial mean wind that undergoes a rather realistic QBO. This MIROC produces perhaps the best "self-consistent" simulation of the QBO of any present-day GCM and so it was used here to study the issue of the QBO response to global warming.

A long control integration of the model was run with observed climatological sea surface temperatures (SSTs) appropriate for the late twentieth century, followed by another integration with increased atmospheric CO_2 concentration and SSTs incremented by the projected twenty-first-century warming in a multi-model ensemble of coupled ocean–atmosphere runs that were forced by the Special Report on Emissions Scenarios (SRES) A1B scenario of future atmospheric composition. In the experiment for late twenty-first-century conditions, the QBO period becomes longer and QBO amplitude weaker than in the late twentieth-century simulation. The downward penetration of the QBO into the lowermost stratosphere is also curtailed in the late twenty-first-

century run. These changes are driven by a significant (30%–40%) increase of the mean upwelling in the equatorial stratosphere. The effect of this enhanced mean circulation overwhelms counteracting influences from strengthened wave fluxes in the warmer climate. The momentum fluxes associated with waves propagating upward into the equatorial stratosphere do strengthen overall by (10%–15%) in the warm simulation; however, the increases are almost entirely in zonal phase-speed ranges that have little effect on the stratospheric QBO but that would be expected to have important influences in the mesosphere and lower thermosphere.

Zonal-mean zonal wind over the equator for (a) present day and (b) double CO₂ conditions. Results shown for pressures between 100 and 5 hPa corresponding to heights of about 17 to 35 km. The color bar is labeled in m/s and the contour interval is 5 m/s.

[Y. Kawatani, K. Hamilton, and S. Watanabe, 2011: The quasi-biennial oscillation in a double CO₂ climate. *J. Atmos. Sci.*, **68**, 265-283, IPRC-737].

Salinity maximum in the North Atlantic

The sea surface salinity (SSS) maximum variability in the North Atlantic was investigated using results from a model of the Consortium for Estimating the Circulation and Climate of the Ocean (ECCO). Salinity budget terms were computed at the model's integration time step and archived as monthly averages. The salinity budget closed, allowing for a mixed-layer salinity budget assessment. The analysis provided the first quantitative evidence for the ocean's role in governing the SSS maximum in the North Atlantic. The results revealed that ocean dynamics explains about half of the SSS variance, being of equal importance as surface forcing. The SSS maximum varies both seasonally and interannually because of interplay among surface flux, advection, and vertical entrainment. The contributions from eddies and small-scale processes are both relatively weak, but not negligible. These results are likely to be useful for the design and interpretation of future observations, especially for the upcoming ocean salinity field campaign, known as Salinity Processes in the Upper-Ocean Regional Study (SPURS) in the North Atlantic, scheduled for

2012–2013. They may also provide a useful baseline for the validation of SSS measurements from the new Aquarius satellite.

[T. Qu, S. Gao, I. Fukumori]

Dynamics of meridional overturning circulation-response to buoyancy forcing and winds

The work on dynamics of the buoyancy-forced meridional overturning circulation (MOC) described in last year's report has been extended by adding an idealized zonal wind that generates a subpolar gyre. Analytical and numerical solutions were obtained to a variable-density, two-layer model and to an OGCM, respectively. The generation of deep water ("sinking") occurs mainly in the interior, poleward flow of the subpolar gyre. The strength of the MOC is not much affected by weak winds, but during strong winds, part of the deep water generated by "sinking" upwells to the upper layer within the subpolar gyre before being exported to low latitudes.

[F. Schloesser, J. P. McCreary, A. Timmermann, and R. Furue]

Estimating ocean mixing in the tropical Pacific

A collaborative project involving researchers from the University of Hamburg, the Scripps Institution of Oceanography, and the University of Hawaii is exploring the effects of oceanic mixing on the large-scale circulation in an eddy-permitting, tropical-Pacific model and working to optimize the mixing field to obtain a model field that best fits observations. In FY2010, the response of the model to changes in vertical diffusivity in various geographical regions was explored. It was found that initially a local response to the changed diffusivity dominates, followed by the propagation of the signal by Rossby waves and Kelvin waves. Off-equatorial vertical diffusivity significantly impacts the equatorial stratification, possibly because of this wave adjustment and/or because diapycnal mixing modifies water parcels while they move equatorward in the Subtropical Cell.

[R. Furue, Y. Jia, J.P. McCreary, K. Richards, N. Schneider and extramural collaborators]

Ocean current striations

Observations of small meridional-scale striations in the zonal ocean current have been described in previous reports. In FY2010 a systematic analysis and cataloguing of time-varying striation features was undertaken using satellite altimetry data and OFES model output. Striations were found to be common in subtropical basins, with the wavelength corresponding to the local deformation radius rather than to the Rhines scale. The striations are most pronounced in regions of low eddy-kinetic energy and normally propagate towards the equator with meridional tilt and phase speed consistent with long non-dispersive baroclinic Rossby waves. Idealized and realistic configurations of the ROMS ocean model have been set up to study the formation processes of the linear and nonlinear beta-plumes, induced by the localized wind stress, transitions between the two regimes, and their relevance to the striations in the eastern North Pacific.

[O. Melnichenko, N.A. Maximenko, A. Reda Bel Madani and colleagues; O. Melnichenko, N.A. Maximenko, N. Schneider, and H. Sasaki, 2010: Quasi-stationary striations in basin-scale oceanic circulation: Vorticity balance from observations and eddy-resolving model. *Ocean Dyn.*, **60**, 653–666; IPRC-666]

Small scale velocity features in the equatorial upper ocean

Small vertical-scale velocity features (SVS) in the near-equatorial upper ocean have been identified in observations and are now being studied in a variety of dynamical models. In the last year, additional high-resolution measurements using a lowered acoustic Doppler current profiler (LADCP) were taken in the western equatorial Pacific aboard R/V Mirai. To complement the LADCP data, turbulent dissipation rates were also measured during this research cruise. On the modeling side, a large number of experiments have been conducted aimed at (i) understanding the development of SVS-forming instabilities in a fully three-dimensional setup; (ii) investigating the possible role of the inertial and parametric subharmonic instabilities in the formation of the SVS features observed during the earlier July, 2008 R/V Mirai cruise; and (iii) exploring an alternative mechanism for generating the SVSs through transient wind events.

[K. Richards and A. Natarov]

Chapter 3: Asian and Global Monsoon System

Inter-monsoon phase relationships

The phase relationships among the western North Pacific summer monsoon (WNPM), the Australian summer monsoon (AM), and the Indian summer monsoon (IM) were investigated using rainfall, SST, and NCEP reanalysis data for the period 1979–2005. A strong WNPM was found often to follow a strong AM but to lead a weak AM, and a significant simultaneous negative correlation appears between WNPM and IM. The in-phase relationship from AM to the succeeding WNPM occurs often during the El Niño decaying phase. The out-of-phase relation from WNPM to the succeeding AM occurs either during the El Niño early onset phase or during the El Nino decaying phase. The simultaneous negative correlation between WNPM and IM often appears either during the El Niño early onset phase when the warm eastern Pacific SSTA induces the cyclonic wind shear that strengthens WNPM but suppresses convection over India, or during the El Niño decaying summer when a weak WNPM results from the persistence of the local anomalous anticyclone and a strong IM results from the El Niño-to-La Niña transition or a basin-wide Indian Ocean warming.

[D. Gu, T. Li, Z. Ji, and B. Zheng, 2010: On the western North Pacific Monsoon, Indian Monsoon and Australian Monsoon phase relations. *J. Clim*., **23**, 5572-5589; IPRC-682]

Upscale feedback of synoptic-scale variability (SSV) to MJO

Two-way interactions between the MJO and SSV were investigated based on NCEP and ERA40 reanalysis data. The observational analyses show that the northwest-southeast oriented synoptic wave train strengthens and is well organized (weakened and loosely organized) in the northwestern Pacific during the enhanced (suppressed) MJO phase. The SSV, on the other hand, may exert an upscale feedback to MJO through 1) the nonlinearly rectification of intraseasonal surface latent heat fluxes, 2) the nonlinear rectification of atmospheric intraseasonal apparent heat and moisture sources, and 3) nonlinear eddy-momentum transport. A new eddy-energetics diagnostic tool that separates the effects of the ISO from the low-frequency background state (LFBS, with periods longer than 90 days) was developed. While the LFBS always contributes positively toward the eddy kinetic energy in boreal summer, regardless of the ISO phases, the synoptic eddies extract energy from the ISO during the ISO active phase but lose kinetic energy to the ISO flow during the ISO suppressed phase. Our diagnosis shows that the nonlinearly rectified surface heat fluxes and apparent heat sources (Q1 and Q2) due to the eddy-mean flow interaction account for 10-30% of the total intraseasonal surface latent heat flux and Q1 and Q2 variabilities over the WNP.

[C. Zhou, and T. Li, 2010: Upscale feedback of tropical synoptic variability to intraseasonal oscillations through the nonlinear rectification of the surface latent heat flux. *J. Clim.,* **23**, 5738-5754; IPRC-693; P.-C. Hsu, T. Li, and C.-H. Tsou: Interactions between boreal summer intraseasonal oscillations and synoptic-scale disturbances over the western North Pacific. Part I: Energetics diagnosis. *J. Clim.,* in press. IPRC-722; P.-C.Hsu, and T. Li: Interactions between boreal summer intraseasonal oscillations and synoptic-scale disturbances over the western North Pacific. Part II: Apparent heat and moisture sources and eddy momentum transport. *J. Clim.,* in press; IPRC-723]

Effect of air-sea coupling on boreal summer ISO (BSISO)

The effects of air-sea coupling over the tropical Indian Ocean (TIO) on the eastward- and northward-propagating BSISO were investigated by comparing a fully coupled (CTL) and a partially decoupled Indian Ocean (pdIO) experiment using the SINTEX-F coupled GCM. Air-sea coupling over the TIO significantly enhances the intensity of both the eastward and northward propagations of the BSISO. The maximum spectrum differences of the northward- (eastward-) propagating BSISO between the CTL and pdIO reach 30% (25%) of their respective climatologic values. The enhanced eastward (northward) propagation is related to the zonal (meridional) asymmetry of a sea surface temperature anomaly (SSTA). A positive SSTA appears to the east (north) of the BSISO convection, which may positively feed back to the BSISO convection. In addition, air-sea coupling may enhance the northward propagation through changes in the mean vertical wind shear and low-level specific humidity. The interannual variations of the TIO regulate the air-sea interaction effect. Air-sea coupling enhances (reduces) the eastward-propagating spectrum during the negative Indian Ocean dipole (IOD) mode, positive Indian Ocean basin (IOB) mode and normal years (during positive IOD and negative IOB years). Such phase dependence is attributed to the role of the background mean westerly in affecting the wind-evaporation-SST feedback. A climatological weak westerly in the equatorial Indian Ocean can be readily reversed by anomalous zonal SST gradients during the positive IOD and negative IOB events. Although the SSTA is always positive to the northeast of the BSISO convection for all interannual modes, air-sea coupling reduces the zonal asymmetry of the low-level specific humidity and thus the eastward propagation spectrum during the positive IOD and negative IOB modes, while strengthening them during the other modes. Air-sea coupling enhances the northward propagation under all interannual modes due to the persistent westerly monsoon flow over the northern Indian Ocean.

[A.-L. Lin, T. Li, X. Fu, J.-J. Luo, and Y. Masumoto: Effects of air-sea coupling on the boreal summer intraseasonal oscillations over the tropical Indian Ocean, *Clim. Dyn.*, in press; IPRC-736]

Effect of the Maritime Continent on MJO propagation

The effect of the Maritime Continent on the propagation characteristics of the boreal summer intraseasonal oscillation (ISO) over the Indo-western Pacific region was investigated by comparing ECHAM5 T159 simulations that either removed or retained the Maritime Continent. A finite domain wavenumber-frequency spectral analysis revealed that the most significant effect of removing the Maritime Continent is the weakening of the northward propagation of the ISO over the Asian monsoon region (65°E-160°E). The diagnosis of the model outputs indicates that the weakening of the northward propagation is primarily due to reduction of the background easterly shear and a low-level southerly and meridional humidity gradient.

[W. Zhu, T. Li, X. Fu, and J.-J. Luo, 2010: Influence of the Maritime Continent on the Boreal Summer Intraseasonal Oscillation. *J. Meteor. Soc. Japan*, **88**, 395-407; IPRC-681]

Extratropical influences on the MJO

Previous studies have claimed that more than 50% of Madden-Julian Oscillation (MJO) events are 'successive', i.e. they can be identified as following a particular preceding event. is influenced by the circumnavigating waves and the extratropics and more than 50% of the MJO In this project a unique global-climate-model (GCM)-based framework was constructed to examine the

role of such preceedign events and in particular to diagnose the relative roles of the circumnavigating waves and forcing from the extratropics on the MJO. In addition to a standard GCM simulation ('control'), several 20-year sensitivity tests were conducted. For example, in the first (second) test, model prognostic variables were relaxed in the tropical Atlantic region (20°-30° latitude zones) toward the 'controlled' climatological annual cycle to remove the influence of the circumnavigating waves (extratropics). The results suggest that the circumnavigating waves do not greatly impact the MJO, whereas the MJO variance was substantially reduced in the absence of extratropical influences. We believe that this is the first effort to quantitatively demonstrate the relative roles of the two processes on the MJO statistics. [

P. Ray, T. Li, and colleagues].

Cause of El Niño and La Niña amplitude asymmetry

The amplitude asymmetry between El Niño and La Niña events was investigated by diagnosing a mixed-layer heat-budget analysis during the developing phases of ENSO. The nonlinear zonal and meridional ocean temperature advection terms are essential to the observed ENSO asymmetry in the eastern Pacific, whereas vertical nonlinear advection reduces the asymmetry. The zonal current anomaly is dominated by the anomalous geostrophic current, which arises from the anomalous thermocline depth associated with the maximum temperature changes. The anomalous meridional current is dominated by the wind-stress-driven current anomaly. The locally enhanced eastward (westward) zonal currents during El Niño (La Niña) result in the anomalous downwelling (upwelling) in the far eastern equatorial Pacific, leading to cold nonlinear vertical advection in both warm and cold episodes.

[J. Su, R. Zhang, T. Li, X. Rong, J. Kug, and C.-C. Hong, 2010: Amplitude asymmetry of El Niño and La Niña in the eastern equatorial Pacific. *J. Clim.*, **23**, 605–617; IPRC-761]
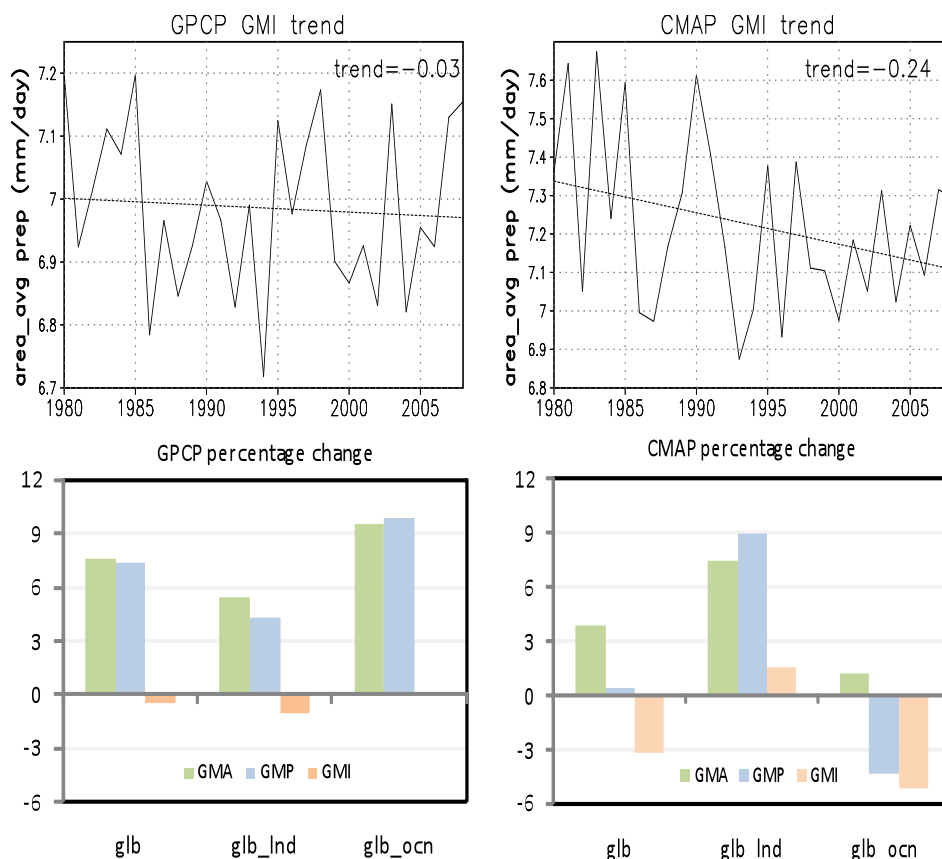
Interdecadal changes in the South China Sea summer monsoon

Analysis of NCEP and ERA40 reanalysis data and Xisha Island station observations indicates that the low-level meridional wind (LLMW) over the South China Sea (SCS) has changed since the late 1970s. The LLMW change is associated with lower tropospheric temperatures in mid-latitude East Asia. An explanation of the tropospheric cooling is as follows. Enhanced convective heating over the southern South China Sea results in a meridional vertical overturning circulation, with anomalous descending motion over continental East Asia. The anomalous descending motion reduces the local humidity through both anomalous low-level divergence and dry vertical advection. The decrease in local tropospheric humidity increases outgoing longwave radiation into space and thus cooler temperatures. The decrease in temperature and thickness leads to anomalous low (high) pressure and convergent (divergent) flows at upper (lower) levels. This further enhances the descending motion and sets up a positive feedback loop.

[C. Li, T. Li, J. Liang, D. Gu, A. Lin, and B. Zheng, 2010: Interdecadal variations of meridional winds in the South China Sea and their relationship with summer climate in China. *J. Clim.*, **23**, 825-841, IPRC-661]

Trends in global monsoon precipitation over the past 30 years

Analysis of the GPCP and CMAP datasets for the past 30 years (1979–2008) indicates consistent increasing trends in both the global monsoon area (GMA) and the global monsoon total precipitation (GMP). This positive monsoon rainfall trend differs from findings of previous studies that assumed a fixed global monsoon domain. Due to the increasing trends in both the GMA and GMP, a global monsoon intensity (GMI) index, which measures the global monsoon precipitation rate per unit area, was introduced. The GMI measures the strength of the global monsoon. Our calculations with both the GPCP and CMAP datasets show a consistent downward trend in the GMI over the past 30 years. This decreasing trend is primarily attributed to a greater percentage increase in the GMA than in the GMP. A further diagnosis reveals that the decrease in the GMI is primarily attributed to the land monsoon in the GPCP, but to the oceanic monsoon in the CMAP.

Top: Linear trends (dashed line) of the global monsoon intensity (GMI, unit: mm/day) in the GPCP (left) and CMAP (right) datasets for the period 1979-2008.
Bottom: Percentage change in the two data sets in the GMA (green), GMP (blue), and GMI (orange): "*glb*" denotes "*global monsoon domain;*" "*glb_lnd*" the *global land monsoon region*; and "*glb_ocn*" the *global oceanic monsoon region*.

[P.-C. Hsu, T. Li, and B. Wang: Trends in Global Monsoon area and precipitation over the past 30 years. *Geophys. Res. Lett.*, in press; IPRC-754]

Future tropical cyclone location shift in Pacific under global warming

Two global high-resolution atmospheric general circulation models (ECHAM5 T319 and HiRAM2.1) were used to investigate the change in tropical cyclone frequency in the North Pacific under global warming. A time-slice method was used in which SST fields derived from either a lower-resolution coupled model run or an ensemble mean SST pattern under the 20C3M (in which historical greenhouse gases in 20th century were prescribed as radiative forcing) and A1B (in which carbon dioxide concentration was increased 1% each year from 2000 to 2070 and then kept constant) scenarios are specified as the lower boundary conditions to simulate the current and the future warming climate, respectively. A significant shift was found in the location of tropical cyclones from the western to central Pacific in both models. The shift to more tropical cyclones in the central and to less in the western Pacific is not attributable to a change in atmospheric static stability, but rather to a change in the variance of tropical synoptic-scale perturbations associated with a change in the background vertical wind shear and boundary-layer divergence.

[T. Li, M. Kwon, M. Zhao, J. Kug, J. Luo, and W. Yu, 2010: Global warming shifts Pacific tropical cyclone location, *Geophys. Res. Lett.*, **37**, L21804, doi:10.1029/2010GL045124, IPRC-720]

Tropical cyclone versus monsoon induced rainfall variability

The interannual variations of tropical cyclone and monsoon induced rainfall in Taiwan were investigated during July–September for the period 1950–2002. To examine the effects of TCs and monsoons, local rainfall was categorized as either TC rainfall (P_{TC}) or seasonal monsoon rainfall (P_{SM}). The former is due to TC passage across Taiwan, while the latter is due to the large-scale monsoon circulation. Two main rainfall patterns that vary from year to year were found: enhanced P_{TC} but suppressed P_{SM} (T+S-) and suppressed P_{TC} but enhanced P_{SM} (T-S+). Physical mechanisms responsible for the two types were examined.

[J.-M. Chen, T. Li, and C.-F. Shih, 2010: Tropical cyclone and monsoon induced rainfall variability in Taiwan. *J. Clim.*, **23**, 4107-4120; IPRC-685]

Quantifying the environmental control on tropical cyclone intensity change

A composite analysis was used to examine environmental, climatological, and persistence characteristics of tropical cyclones (TCs) undergoing different forms of intensity changes in the western North Pacific (WPAC) and North Atlantic (ATL) ocean basins. The cumulative distribution functions of 24-h intensity changes from the 2003–08 best-track data were categorized as follows: rapidly intensifying (RI), intensifying, neutral, and weakening. For the environmental variables, statistically significant differences were examined between RI storms and the other groups. While some environmental differences were found between RI and weakening/neutral TCs in both basins, an interesting result from this study is that the environment of RI TCs and intensifying TCs is quite similar. This indicates that, provided the environment is favorable, the rate of intensification depends on average only weakly on environmental conditions. In the ATL, RI events occurred in environments with weaker deep-layer shear than intensifying events. Moreover, the SSTs for intensifying and rapidly intensifying TCs are similar, indicating that the rate of intensification is not critically dependent on SST. The TCs in both

basins were more intense prior to undergoing an RI episode than an intensifying or neutral episode.

[E.A. Hendricks, M. S. Peng, B. Fu, and T. Li, 2010: Quantifying environmental control on tropical cyclone intensity change. *Mon.Wea.Rev*., 138, 3243-3271; IPRC-758]

Amplitude asymmetry of the Indian Ocean basin mode

A basin-wide warming (cooling) in the Indian Ocean is observed following the El Niño (La Niña) mature phase, with the amplitude of the warming being significantly larger than the cooling. A composite analysis reveals that the amplitude asymmetry (positive skewness) between the warm and cold Indian Ocean basin-wide SSTA pattern appears only when ENSO is concurrent with the Indian Ocean Dipole (IOD). The physical mechanism for the amplitude asymmetry is investigated by analyzing the mixed-layer heat budget based on SODA 2.0.2 data. It is found that the positive skewness in the west pole is mainly associated with the asymmetry of ocean temperature advections, whereas the positive skewness in the east pole is associated with the asymmetry of the surface heat flux anomaly (primarily shortwave radiation) in response to the ENSO remote forcing.

[C.-C. Hong, T. Li, H. Lin, and Y.-C. Chen, 2010: Asymmetry of the Indian Ocean Basin-wide SST Anomalies: Roles of ENSO and IOD. *J. Climate*, **23**, 3563–3576. doi: 10.1175/2010JCLI3320.1; IPRC-674]

Asymmetric SSH–SST relationship in positive and negative IOD events

The sea surface height (SSH)-sea surface temperature (SST) relationship in the eastern equatorial Indian Ocean (EEIO) displays a significant asymmetry between the positive and negative SSH anomalies in boreal autumn. Whether the thermocline-SST feedback is responsible for the negative SST skewness in the EEIO was explored by diagnosing various air-sea feedback processes and a mixed-layer heat budget. The observational analysis shows that the SSH-subsurface temperature relation is approximately symmetric between the positive and negative episode, implying that the observed SSH-SST asymmetry is not attributable to ocean thermocline feedback. A further analysis of the SST–precipitation, precipitation–wind stress and wind stress–SSH relations indicates that the asymmetry arises from asymmetric atmospheric heating/wind responses to the SST anomaly. A mixed-layer heat budget analysis reveals that the ratio of the mixed-layer temperature tendency between the positive and negative events is not affected by changes in vertical temperature advection, suggesting that the thermocline-feedback is not crucial for generating the negative SST skewness in the EEIO.

[Hong, C.-C., and T. Li, 2010: The independence of SST skewness to thermocline feedback in the eastern equatorial Indian Ocean. *Geophys. Res. Lett.*, **37**, L11702, doi:10.1029/2010GL043380.]

Effect of the mean state on IOD development

Boreal summer is the critical season for rapid development of the Indian Ocean Dipole (IOD). In this study, three factors related to the boreal summer mean state and possibly contributing to rapid IOD development were examined 1) As part of the Indo-Pacific warm pool, the high mean SST in the southeastern tropical Indian Ocean (SEIO) acts as an essential prerequisite for the development of anomalous convection. 2) The maximum suppressed precipitation in response to a cold SST anomaly (SSTA) in the southern equatorial IO shifts northward towards the equator

because the mean precipitation is equatorially trapped in boreal summer. 3) The monsoonal easterly shear in boreal summer promotes a more equatorially symmetric low-level Rossby wave response to a prescribed equatorially asymmetric heating over the southern equatorial IO. The above three processes strengthen the equatorial zonal wind anomaly and thus the Bjerknes feedback, as well as the IOD development during boreal summer.

[Xiang, B., W. Yu, T. Li, and B. Wang, 2011: The critical role of the boreal summer mean state in the development of the IOD. *Geophys. Res. Lett.*, in press]

Diagnostic metrics for evaluating the annual and diurnal cycles in global models

We proposed two sets of diagnostic metrics for evaluating the simulation of the forced response to annual and diurnal cycles of solar radiation in global models. The metrics for the annual cycle (AC) variation include the annual mean, the solstice and equinoctial asymmetric modes, and the global-monsoon precipitation domain and intensity. The metrics for the diurnal variation include the diurnal range, the land-sea contrast and transition modes of the diurnal cycle (DC), and the diurnal peak propagation in coastal regions. The proposed modes for the AC and DC represent faithfully the first two leading empirical orthogonal functions and explain, respectively, 82% of the total annual variance and 87% of the total diurnal variance over the globe between 45°S and 45°N. The simulated AC and DC by the 20-km-mesh MRI/JMA atmospheric general circulation model (AGCM) considerably outperforms any single AMIP II GCM and performs comparable to 12-AMIP II model ensemble simulation as measured by Pearson's pattern correlation coefficient. Comparison of four versions of the MRI/JMA AGCM with increasing resolution (180, 120, 60, and 20 km) reveals that the 20-km version reproduces the most realistic annual and diurnal cycles. However, the improved performance is not a linear function of the resolution. Marked improvement of the simulated DC (AC) occurs at the resolution of 60 km (20 km). The common deficiencies in representing the monsoon domains suggest the models have difficulty in replicating the annual march of the subtropical high, which is largely driven by prominent east-west land-ocean thermal contrasts. Note also that the 20-km model reproduces a realistic diurnal cycle, but fails to capture realistically the Madden-Julian Oscillation.

[B. Wang, H.-J. Kim, K. Kikuchi, and A. Kitoh: Diagnostic metrics for evaluation of annual and diurnal cycles. *Climate Dyn.*, in press; IPRC-709]

Spring Eurasian snow cover and East Asian summer monsoon

The Eurasian snow-cover anomalies in spring are thought to affect East Asian summer monsoon (EASM). The spring snow-cover data for the period from 1972 to 2004 were used to extract dominant spatial patterns over the Eurasian region and to examine their impacts on the EASM through empirical orthogonal function (EOF) analysis. The first EOF mode is largely characterized by a continent‑wide snow-cover anomaly over the whole Eurasian region, while the second EOF mode is dominated by an east‑west dipole structure over Eurasia. Our study indicates that the dipole patterns of snow cover are more closely related to EASM rainfall variations than continent‑wide snow cover. A strong dipole pattern with positive (negative) snow-cover anomalies over western Eurasia and negative (positive) snow-cover anomalies over eastern Eurasia is associated with enhanced (reduced) summer rainfall over East Asia, and the Eurasian wave train pattern is apparent. An important implication of these results is that the spring snow-cover anomalies over Eurasia are precede EASM rainfall anomalies.

[S.-Y. Yim, J.-G. Jhun, R. Lu, and B. Wang, 2010: Two Distinct Patterns of Spring Eurasian Snow Cover Anomaly and Their Impacts on the East Asian Summer Monsoon. *J. Geophys. Res*., **115**, D22113, 10 PP., doi:10.1029/2010JD013996; IPRC-731]

Future change in tropical cyclone tracks: Projections in a 20-km-mesh global atmospheric model

Possible future change in tropical cyclone (TC) activity over the North Atlantic (NA) was investigated by comparing 25-year simulations of present-day and future climate under the A1B emission scenario using a 20-km mesh atmospheric general circulation model from the Meteorological Research Institute and Japan Meteorological Agency. The present-day simulation reproduces many essential features of observed climatology and interannual variability in TC frequency and tracks over the NA. For the future projection, the model is driven by sea surface temperature (SST) trend projected by the most recent Intergovernmental Panel for Climate Change (IPCC) multi-model ensemble and year-to-year SST variations derived from present-day climate. A major finding is that *the frequency of TCs in the NA will not change significantly, but they will decrease in the tropical western NA (WNA) and increase in the tropical eastern NA (ENA) and northwestern NA (NWNA).* The projected change in TC tracks suggests *a reduced probability of TC landfall over the southeast US but an increased probability over the northeast US.* The track changes are not due to changes in the large-scale steering flows but due to a shift in TC genesis locations. The increased TC genesis in ENA arises from increasing background ascending motion and convective available potential energy. In contrast, the reduced TC genesis in the WNA is attributed to decreases in mid-tropospheric relative humidity and ascending motion caused by remotely forced anomalous descent. This finding indicates that the impact of remote dynamical forcing is greater than that of local thermo-dynamical forcing in the WNA. The increased frequency of TC occurrence in the NWNA is attributed to reduced vertical wind shear and the pronounced local warming of the ocean surface. These TC changes appear to be most sensitive to projected changes in the spatial distribution of rising SST. Given that most IPCC models project a larger increase in SST in the ENA than in the WNA, the simulated projected eastward shift in TC genesis is likely to be robust.

[Murakami, H., and B. Wang, 2010: Future change of North Atlantic tropical cyclone tracks: Projection by a 20-km-mesh global atmospheric model. *J. Clim*., **23**, 2699-2721; IPRC-679]

Bimodal representation of the tropical intraseasonal oscillation

The tropical intraseasonal oscillation (ISO) shows variability centers and propagation patterns that differ distinctly between boreal winter and summer. To accurately represent the state of the ISO at any particular time of the year, a bimodal ISO index was developed. It consists of the Madden-Julian Oscillation (MJO) with predominant eastward propagation along the equator and the Boreal Summer ISO (BSISO) with prominent northward propagation and large variability in off-equatorial monsoon-trough regions. The spatial-temporal patterns of the MJO and BSISO were identified in an extended empirical orthogonal function analysis of 31 years (1979–2009) OLR data for the December–January–February and the June–July–August period, respectively. The dominant mode of the ISO at any given time can be judged by the proportions of the OLR anomalies projected onto the two type of oscillations. The bimodal ISO index provides objective and quantitative measures on the annual and interannual variations of the predominant ISO modes. From December through April the MJO mode dominates while from June through

October the BSISO mode dominates. May and November are transitional months when the predominant mode changes from one to the other. Moreover, the fractional variance reconstructed from the bimodal index is significantly higher than the counterpart reconstructed from the Wheeler and Hendon index. The bimodal ISO index also shows excellent real-time monitoring skill. The method and results provide critical information for assessing models' abilities to reproduce the ISO, for developing further research on the predictability of the ISO and for a variety of scientific and practical purposes.

[K. Kikuchi, B. Wang, Y. Kajikawa: Bimodal representation of the tropical intraseasonal oscillation, submitted to *Clim. Dyn*.]

Tropical cyclogenesis in the Northern Indian Ocean associated with the tropical intraseasonal oscillation

Over the northern Indian Ocean (NIO), a substantial number (~60%) of tropical cyclones (TCs) form in association with significant intraseasonal oscillation (ISO) events (e.g., Nargis [2008]). In this paper, the relationship between TC genesis and ISO in the NIO was studied using 30-year (1979–2008) observations. Because NIO TCs mainly occur in transitional seasons when climatological environmental forcing favors TC genesis, two types of ISO modes, the northward-propagating boreal summer intraseasonal oscillation (BSISO) and the east-ward propagating Madden-Julian oscillation (MJO) representing the boreal winter ISO, were objectively and quantitatively defined, and their connection with TC genesis was examined. It was found that over 70% of ISO-related genesis is associated with the BSISO mode and up to 30% with the MJO mode. The BSISO mode primarily affects TC formation in May–June and September–November, whereas the MJO mode affects TC formation primarily in November–December. Because of their distinct structures and lifecycles, the BSISO and MJO modes affect TC formation differently. The BSISO mode increases the probability of TC formation during its wet phases over the NIO. The MJO mode increases the probability of TC formation after the convection passes over the Malay Peninsula and when the Indian Ocean is in a dry phase. The BSISO mode increases TC genesis probability by creating favorable environmental forcing for TC genesis, whereas the MJO mode does not. The most salient feature is that both the ISO modes favor TC genesis by providing a synoptic-scale seeding disturbance at least six days prior to TC formation. The seeding disturbance provided by the BSISO is a cyclonic vorticity anomaly to the north of the equatorial convection/westerly wind burst, whereas the seeding provided by the MJO is a convectively coupled Rossby wave that breaks away from the major body of the MJO convection. The seasonality of the NIO TC genesis, intensity, and prevailing tracks are also explained in terms of the effect of environmental forcing on TC genesis potential, steering flow, and maximum potential intensity. The results imply that monitoring the evolution of the two types of ISO modes, especially the BSISO, may improve medium-range forecasts for NIO cyclogenesis.

[Kikuchi, K. and B. Wang, 2010: Formation of tropical cyclones in the northern Indian Ocean associated with two types of tropical intraseasonal oscillation modes. *J. Meteor. Soc. Japan*, **88,** 475-496.]

Effect of land-surface processes on extended monsoon breaks

Analysis of a 50-year control run of AM2.1 forced with climatological SST but with land-atmosphere interaction showed the successful simulation of extended monsoon breaks over south

Asia. Another 50-year simulation forced with climatological SST but in which land-atmosphere interaction was NOT allowed was conducted. The results of this latter study are being analyzed.

[H. Annamalai and colleagues]

Dynamical intraseasonal prediction

On account of sparse in-situ observations over the tropical Indo-Pacific region and model deficiencies in the simulation of the tropical intraseasonal oscillations (ISO), reanalysis datasets have various biases in describing the ISO. In this study, we revealed that the equatorial eastward-propagating ISO has been systematically underestimated in NCEP R1, R2, and ERA Interim reanalyses. A signal-recovering method has been proposed to improve the ISO signals in these reanalyses. The intraseasonal prediction skills initialized with signal-recovered reanalyses are systematically higher than those initialized with original reanalyses. The useful skills for 850-hPa zonal winds and precipitation rate over Southeast Asia reach 23 and 18 days.

[X. Fu, B. Wang, J.-Y. Lee, W.Q. Wang, and L. Gao: Sensitivity of dynamical intra-seasonal prediction skills to different initial conditions. *Mon. Wea. Rev.*, in press; IPRC-783]

Extended-range ensemble forecasting of tropical cyclone Nargis (2008)

A conventional atmosphere-ocean coupled system initialized with the NCEP FNL analysis product successfully predicted the genesis of tropical cycle Nargis (2008) with a lead time of two weeks. The coupled forecasting system reproduces the westerly wind bursts in the equatorial Indian Ocean associated with an eastward-propagating Madden-Julian Oscillation (MJO) event as well as the accompanying northward-propagating westerly and convective disturbances. After reaching the Bay of Bengal, this northward-propagating Intra-Seasonal Variability (ISV), fosters the genesis of tropical cyclone Nargis. The finding demonstrates that a realistic MJO/ISV prediction will make the extended-range forecasting of tropical cyclone genesis possible and calls for improved representation of the MJO/ISV in contemporary weather and climate forecast models.

[X. Fu, and P.-C. Hsu]

Tropical intraseasonal rainfall variability in various reanalyses

This study analyzed tropical intraseasonal rainfall variability in the recently completed NCEP Climate Forecast System Reanalysis (CFSR) and its comparison with the widely used NCEP R1and R2. The R1 produces too little rainfall variability while the R2 generates too strong a westward propagation. Compared with the R1 and R2, the CFSR produces greatly improved tropical intraseasonal rainfall variability with a more realistic dominating eastward propagation and more realistic amplitude. Rainfall variability from the other two recently produced reanalyses, the ECMWF Re-Analysis Interim (ERAI) and the Modern Era Retrospective-analysis for Research and Applications (MERRA), were also analyzed. Both the ERAI and MERRA generate stronger rainfall spectra than the R1 and more realistic dominance of eastward propagating variance than R2. The intraseasonal variability in MERRA is stronger than that in the ERAI but weaker than that in the CFSR.

[J. Wang, J., Wang, X. Fu, K.H. Seo, Tropical intraseasonal rainfall variability in CFSR, *Clim. Dyn.,* in press; IPRC-780]

Data assimilation improves weather analysis and rainfall prediction

The Tropical Warm Pool–International Cloud Experiment (TWP–ICE) collected extensive ship and aircraft observations in northern Australia during January and February 2006. In this study, additional sounding observations collected during the experiment were included to further analyze the characteristics of weather systems and associated environmental conditions during four different regimes: active wet monsoon, suppressed dry monsoon, clear day, and monsoon break. Monsoon low-pressure systems dominate during the active wet monsoon and monsoon break periods. In the active monsoon system, heavy rainfall (>100 mm day^{-1}) occurs over the tropical ocean of northern Australia and Tiwi Island, where under the influence of the monsoon low, low-level southerly-to-southwesterly winds dominate over the ocean. During the suppressed monsoon period and clear days, the environment is very dry under the influence of the monsoon ridge when conditions unfavorable for convection and rainfall prevail. During the suppressed monsoon, the dry air intrusion into the mid-troposphere has its driest center around 600-hPa and is related to dry-air advection from subtropical regions and subsidence associated with an approaching monsoon ridge. The typical westerly winds prevail between 850 and 700 hPa in Darwin. The driest period during 2006 TWP–ICE occurred during clear days, when there was subsidence related to the monsoon ridge. Thus in contrast to the NCEP/FNL global analysis, the assimilation of additional sounding data collected in the field experiment of TWP–ICE allowed clear identification of the dominant weather systems during the four types periods. The daily rainfall predictions also improved during the IOP, especially in the active monsoon period.

[H.-C. Yeh, and X. Fu: Application of Additional Sounding Observations on Weather Analysis and Rainfall Prediction during Intensive Observing Period of 2006 TWP-ICE. *Terr. Atmos. Ocean. Sci.*, in press; IPRC-776]

Coupled model prediction of summertime teleconnection

The retrospective forecast skill of three coupled climate models (NCEP CFS, GFDL CM2.1 and CAWCR POAMA 1.5) and their multi-model ensemble (MME) was evaluated by analyzing the predictable modes of the Northern Hemisphere (NH) summer upper-tropospheric circulation along with the relevant monsoon precipitation anomalies for the 25-year period of 1981–2005. The seasonal prediction skill for the NH 200-hPa geopotential height comes from the coupled models' ability to predict the first two empirical orthogonal function (EOF) modes of the interannual variability; the models cannot replicate the residual higher modes. The long-lead predictability of the EOF1 comes mainly from the prolonged impacts of El Niño as the EOF1 tends to reflect conditions during the summer after the mature phase of El Niño. The EOF2, in contrast, is related to the developing El Niño and also the interdecadal variability of the sea surface temperature over the North Pacific and the North Atlantic Ocean. In both observation and the one-month lead MME prediction, the first two leading modes are accompanied by significant rainfall and surface air temperature anomalies in the continental regions of the NH extratropics. The MME's success in predicting the EOF1 (EOF2) is likely to lead to better prediction of JJA precipitation anomalies over East Asia and the North Pacific (central and southern Europe and western North America).

[J.-Y. Lee, B. Wang, Q. Ding, K.-J. Ha, J.-B. Ahn, A. Kumar, B. Stern, and O. Alves: How predictable is the northern hemisphere summer upper-tropospheric circulation? *Clim. Dyn.* doi:10.1007/s00382-010-0909-9, in press; IPRC-622]

Improvement of the APCC Probabilistic Multi-Model Seasonal Prediction

Efforts have been devoted to improving a probabilistic multi-model prediction (PMMP) system of the Asia-Pacific Economic Cooperation (APEC) Climate Center (APCC). This system, consisting of seven two-tier and three one-tier prediction models, has been used for the APCC operational seasonal climate forecast. The PMMP, targeting one-month lead, tercile-categorical probabilistic seasonal forecast for temperature and precipitation, was first established with retrospective forecast (hindcast) for the 23 years from 1981 to 2003 and then used for real-time forecast from 2008 to 2010. The novelty of the improved PMMP system is the use of an upgraded multivariable version of a stepwise pattern projection method (SPM) in conjunction with a quantification of forecast uncertainty due to models' systematic errors in terms of probabilities. This approach was shown to improve the reliability and resolution of the PMMP forecast skill for temperature and precipitation in June-July-August (JJA) for both cross-validated hindcast and independent real-time forecast periods. The new PMMP has the area-averaged relative operating characteristic (ROC) score of 0.7 (0.65) for JJA temperature (precipitation) in cross-validation of the hindcast, while the uncalibrated raw-models' PMMP has a ROC score of 0.63 (0.56).

[Y.-M. Min, J.-Y. Lee, J.-S. Kug, B. Wang, and colleagues: Improvement of the APCC probabilistic multi-model seasonal prediction by systematic error correction and uncertainty estimation. submitted to *Clim. Dyn*.]

Climatologic subseasonal variations in the North Pacific and Atlantic

Using NCEP-2 reanalysis data for the period 1979–2008, differences in the storm track–jet stream relationship over the North Pacific and over the North Atlantic were investigated in terms of barotropic and baroclinic energetics. Pacific storm-track (PST) activity weakens and follows the southward shift of the Pacific jet from fall to winter, whereas the Atlantic storm-track (AST) activity intensifies but remains in its position regardless of the slight southward shift of the Atlantic jet. In the North Atlantic, meridionally elongated eddies gain kinetic energy efficiently from a stretching deformation of the mean flow in the jet entrance. In contrast, shearing deformation is important for the initiation of PST activity. Analysis of baroclinic energetics reveals that the intensification of the AST activity in midwinter is mainly attributed to coincidence between the location of maximum poleward and upward eddy heat fluxes and the location of the largest meridional temperature gradient slightly upstream of the storm track. The relatively large amount of precipitable water and meridional eddy moisture flux along the baroclinic energy-conversion axis likely provides a more favorable environment for baroclinic eddy growth over the North Atlantic than over the North Pacific. In the meantime, the midwinter minimum of the PST activity is due to the southward shift of the Pacific jet stream that shifts the core region of the poleward and upward heat fluxes away from the meridional thermal gradient.

[S.-S. Lee, J.-Y. Lee, B. Wang, F.-F. Jin, W.-J. Lee, and K.-J. Ha: A comparison of climatological subseasonal variations in the wintertime storm track activity between the North Pacific and Atlantic: local energetics and moisture effect. *Clim. Dyn.* doi: 10.1007/s00382-011-1027-z, in press, IPRC-750]

ENSO Regulation of MJO teleconnection

The extratropical teleconnections associated with the Madden-Julian Oscillation (MJO) were shown to have an action center in the North Pacific, when the pressure anomalies between Phase 3 (convective Indian Ocean) and Phase 7 (convective western Pacific) of the MJO have opposite polarities. The teleconnection in the same phase of the MJO may induce opposite anomalies over East Asia and North America during El Niño and La Niña years. In MJO Phase 3 during La Niña, a gigantic North Pacific anticyclonic anomaly occurs, making coastal northeast Asia warmer and wetter than normal, but the western US colder and drier; during El Niño the anticyclonic anomaly is confined to the central North Pacific, and the northwest US experiences warmer than normal weather under the influence of a downstream cyclonic anomaly. In Phase 7 during La Niña, an extratropical cyclonic anomaly forms over the northwest Pacific due to strengthened convection over the Philippine Sea, producing a bitter winter monsoon over Japan; during El Niño, the corresponding cyclonic anomaly shifts to the northeast Pacific because of enhanced convection over the equatorial central Pacific, which causes warm and wet conditions along the west coast of US and Canada. Although the presence of ENSO-induced seasonal anomalies can significantly modify the MJO teleconnection, it can still be well identified. During Phase 3, the MJO teleconnection pattern over the North Pacific is counterbalanced (enhanced) by El Niño (La Niña)-induced seasonal mean anomalies. During Phase 7, on the other hand, the MJO teleconnection anomalies in the northeastern Pacific will be enhanced during El Niño but reduced during La Niña; the impact of the MJO teleconnection on the North America is, therefore, expected to be stronger during El Niño than during La Niña.

[J.-Y. Moon, B. Wang, and K.-J. Ha, *Climate Dynamics,* in press; IPRC-715]

Interdecadal changes in Northern Hemisphere storm-track activity

Interdecadal changes in storm-track activity and mean flow – transient eddy interaction were investigated using 1948–2009 NCEP-NCAR I and 1958–2001 ECMWF ERA-40 reanalysis data. The analysis reveals three significant interdecadal changes in storm-track activity. First, the most remarkable change in the North Pacific (PST) and North Atlantic storm-track (AST) activity occurred in the early-to-mid 1970s and was characterized by global intensification. Second, the PST activity in midwinter changed significantly from a weak regime during the early 1980s to a strong regime during the late 1980s. This intensification did not appear in the AST. Third, in the recent decade, the PST intensity has increased, especially in early spring, whereas the AST intensity has weakened since the late 1980s.

[S.-S. Lee, J.-Y. Lee, B. Wang, and K.-J. Ha, 2011: Interdecadal change in the storm track intensity and its relationship with energetics. submitted to *Clim Dyn*.]

Cool weather conditions in 2009 over Asia and America

Cool weather conditions hit northern Central and East Asia and central North America in 2009 combined with abundant precipitation, a strong jet stream and prominent meandering upper-level circulation despite the fact that the year 2009 is the fifth warmest year globally in the modern record. The 2009 summer was found to be a unique case of synchronized El Niño development, negative phase of the circumglobal teleconnection (CGT) and the Arctic Oscillation (AO), severely dry Indian summer monsoon (ISM), but abundant Western North Pacific summer

monsoon (WNPSM) rainfall. The strong negative CGT pattern that was associated with the lack of ISM rainfall and the developing El Niño was the main contributor to the cold June whereas the unprecedented negative AO and Pacific-Japan (PJ) or western Pacific-North America (WPNA) teleconnection linked to abundant WNPSM rainfall contributed to the cold July in the above mentioned regions. It is further noted that increased storm-track activity and frequent cold surges from high latitude contributed greatly to the cool and wet summer.

[K.-J. Ha, J.-E. Chu, J.-Y. Lee, B. Wang, S.N. Hameed, and M. Watanabe]

Chapter 4: PALEOCLIMATE

Reconstructing interannual ENSO-related rainfall variability in East Africa

Analysis of the annual thickness and color of sediment layers in Lake Challa, East Africa, permitted a reconstruction of the history of equatorial East African rainfall back in time to the Last Ice Age. The layers are testimony that rainfall in East Africa changed dramatically over the past 21,000 years. During the coldest period 18,000 to 21,000 years ago, the climate was dry and relatively stable. Even though rainfall did not vary much during that period, the sediment layers still reflect the beat of El Niño and La Niña cycles. Compared with this coldest time, the last 3,000 years have been wetter, but more variable with severe century-long droughts sprinkled throughout. Climate model simulations support the forward extrapolation from these lake-sediment data that future Indian Ocean warming will intensify East Africa's hydrological cycle and its inter-annual variability in rainfall.

[C. Wolff, G. Haug, A. Timmermann, J.S.S. Damste, A. Brauer, D.M. Sigman, M.A. Cane, D. Verschuuren, 2011: Reduced rainfall variability in East Africa during the last ice age, submitted to *Science*]

The effect of glacial ocean circulation changes on pCO_2

A series of Last Glacial Maximum (LGM) marine-carbon-cycle sensitivity experiments was conducted to test the effect of different physical processes on atmospheric pCO_2 as simulated by two atmosphere-ocean general circulation model (AOGCM) experiments. One AOGCM solution exhibits an increase in North Atlantic Deep Water (NADW) formation, whereas the other mimics an increase in Antarctic Bottom Water (AABW) associated with a weaker NADW. On account of enhanced gas solubility associated with lower sea surface temperature, both experiments generate a reduction in atmospheric pCO_2 by about 20–23 ppm. However, neither a weakening of NADW nor an increase in AABW formation causes a large atmospheric pCO2 change. A marked increase in AABW formation is required to represent the reconstructed vertical gradient of dissolved inorganic carbon (DIC) during LGM conditions. The efficiency of Southern Ocean nutrient uptake decreases in response to enhanced AABW formation, which counteracts the circulation-induced ocean carbon uptake.

[M. Chikamoto, A. Abe-Ouchi, A. Oka, R. Ohgaito, A. Timmermann, 2011: Glacial marine carbon cycle sensitivities to Atlantic ocean circulation reorganization by coupled climate climate model simulations, in preparation].

Glacial climate instability associated with the closing of the Bering Seaway

Abrupt climate transitions, known as Dansgaard-Oeschger events, occurred during the last glacial period, especially from 80 to 11 thousand years before present, but they were nearly absent during interglacial periods and the early stages of glacial periods, when major ice-sheets were still forming. Using a high-resolution fully coupled state-of-art climate model CCSM3 we demonstrated that shoaling of the Bering Strait and reducing its throughflow between the Pacific and the Arctic Ocean during the glacial period lead to the emergence of stronger hysteresis behavior of the ocean conveyor belt circulation, thus creating conditions that are more conducive to triggering abrupt climate transitions.

[A. Hu, G.A. Meehl, W. Han, A. Timmermann, B. Otto-Bliesner, Z. Liu, W.M. Washington, W. Large, A. Abe-Ouchi, M. Kimoto, K. Lambeck, B. Wu, 2011: The Bering Strait and glacial climate stability, submitted to *Scienc*e]

Obliquity effects on Southern Hemispheric climate

The effect of changes in earth's obliquity on Southern Hemisphere climate was studied using an earth system model of intermediate complexity and a coupled general circulation model. It was shown that phases of low obliquity enhance the meridional temperature gradient, increase the atmospheric baroclinicity and intensify the Southern Hemisphere Westerlies and storm tracks. Transient climate simulations with the earth system model of intermediate complexity that cover the forcing history of the last 130,000 years, demonstrated that the meridional heat transport associated with the orbitally paced modulation of the Westerlies and storm tracks negatively feeds back on Antarctic temperatures and partly offsets the effects of the direct obliquity forcing in Antarctica, thereby creating a high correlation between CO_2 radiative forcing and Antarctic temperature. A balance among shortwave obliquity forcing, atmospheric heat transport changes, and greenhouse gas forcing hence determines the overall timing of temperature changes in Antarctica. A transient modeling experiment with constant CO_2 concentrations further demonstrates that the Southern Hemisphere Westerlies are primarily modulated by the obliquity cycle rather than the CO_2 radiative forcing. By comparing our modeling results with reconstructed dust fluxes in Antarctica, we find that the timing of the major observed dust-peaks during the last 130 kyr is largely determined by the obliquity modulation of Southern Hemisphere Westerlies and storm tracks. Our results challenge hypotheses that invoke winds as a primary driver for glacial-interglacial CO_2 variations.

[A. Timmermann, T. Friedrich O. Elison Timm, A. Abe-Ouchi, 2011, Obliquity effects on Southern Hemispheric westerlies and Antarctic temperatures, in preparation]

Deglacial climate change: reconstructions and transient model simulations

The responses of North Pacific intermediate and deep water ventilation and ocean biogeochemical properties to a northern North Atlantic glacial freshwater perturbation were evaluated with the coupled atmosphere-ocean general circulation model MIROC and the earth system model of intermediate complexity LOVECLIM. When the Atlantic meridional overturning circulation (AMOC) weakens in response to the North Atlantic freshwater discharge, both models simulate a subthermocline and intermediate water warming in the Pacific Ocean. The sensitivity of the Pacific meridional overturning circulation (PMOC) to the AMOC weakening, however, is very different in the two models. MIROC simulates only a small increase in the deep sinking branch of the PMOC in the North Pacific, whereas the LOVECLIM freshwater experiment exhibits intensified deep-water formation in the North Pacific, associated with a transport increase up to 19 Sv. Despite the large differences in their ocean circulation response, both models succeed in reproducing the high-oxygen and low-nutrient conditions of intermediate to deep waters, which are in accordance with sediment-core based paleo-proxy reconstructions from the North Pacific and Bering Sea during Heinrich Event 1. This suggests that the emergence of younger intermediate than deep water in the North Pacific can be partly attributed to an intensified PMOC and partly to enhanced mixing. Our models capture the broad features observed in several paleo-proxy data of the Pacific Ocean: the biological production

decrease off northern Japan, the cooling in the western North Pacific Ocean, and the southward shift of the Pacific Intertropical Convergence Zone.

[M. Chikamoto, L. Menviel, A. Abe Ouchi, R. Ohgaito, A. Timmermann, Y. Okazaki, N. Harada, A. Oka, 2011: Variability of North Pacific Intermediate-Deep Water ventilation during Heinrich events in two coupled models, *Deep Sea Res. II*, submitted]

In a second study, we determined sea surface and subsurface temperatures in the Okhotsk Sea during the Last Glacial Maximum (LGM) and the last deglaciation from measurements of alkenones and from the TetraEther indeX consisting of 86 carbon atoms (TEX86) in piston core sediments, which reveal the region's climate response to global climate changes. The TEX86-derived temperatures differ from the alkenone-derived temperatures from the same and nearby sediment samples in the Okhotsk Sea. This suggests that the different proxies reflect different aspects of thermal-structure changes during the LGM and the last deglaciation. During the LGM, alkenone-derived temperatures in the Okhotsk Sea were relatively warm, a finding at many other sites in the western North Pacific that may reflect the shift in the season and depth of biomarker production from early summer and autumn to midsummer because of expansion of the sea-ice cover season. During the last deglaciation, alkenone-derived temperatures changed in response to the millennial-scale climate change; from 19–10 kyr BP the temperatures were higher during Heinrich Event 1 (H1; 4.1–14.2 C) and Younger Dryas (YD; 6–11.9 C) and lower during the Bølling–Allerød (B–A; 4.8–11.6 C). The apparent warmer alkenone-derived temperatures during the cold events (H1 and YD) may stem from a similar source as during the LGM. Empirical Orthogonal Function (EOF) analysis also indicated a shift in the alkenone production season as the first principal component. The EOF analysis further implied that the alkenone-derived temperature traced the precessional cycle of fall insolation at 45N and millennial time-scale variability in the North Atlantic. The millennial-scale response of alkenone-derived temperatures was probably related to the equatorward (polarward) migration of the westerly jet axis and to the weakened (strengthened) Asian summer monsoons resulting in colder and drier (warmer and wetter climates) in East Asia, including the Okhotsk Sea. Because the Okhotsk Sea and adjacent seas are the source region of North Pacific Intermediate Water, the change in sea-surface temperature and salinity conditions in this region in response to climate changes across millennial time scales would influence the ventilation rate at intermediate-depth layers.

[N. Harada, N., M. Sato, Y. Nakamura, K. Kimoto, Y. Okazaki, K. Nagashima, O. Seki, H. Moossen, J. Bendle, A. Ijiri, T. Nakatsuka, L. Menviel, M. O. Chikamoto, A. Timmermann, A. Abe-Ouchi, 2010" Sea surface and subsurface temperature changes in the Okhotsk Sea and adjacent North Pacific during the last Glacial Maximum and deglaciation, *Deep Sea Research II*, submitted]

A third study investigated the characteristics of the last glacial termination, including its millennial-scale variability, in an Earth system model of intermediate complexity forced by continuously varying boundary conditions and a hypothetical profile of freshwater forcing. The model simulates Heinrich event 1 (H1), the Bølling warm period, the Older Dryas, the Antarctic Cold Reversal (ACR) and the Younger Dryas in close agreement with paleo-proxy data from different regions worldwide. It was found that the ACR was simulated as the bipolar seesaw response to the AMOC recovery during the termination of H1. Our study also suggests that the amplitude of the ACR is amplified by a rapid deglacial partial retreat of the Antarctic icesheet.

We argue that melting from both the Laurentide and the Antarctic Ice sheets contributed to the sea level rise associated with Meltwater Pulse 1-A (MWP1A). It is hypothesized that the Northern Hemisphere source of MWP1A caused the Older Dryas cooling there, whereas the Southern Hemisphere source contributed to the ACR. Our results also document that for the majority of paleo-climate proxies the transient modeling experiments can qualitatively reproduce the relative timing.

[L. Menviel, A. Timmermann, E.O. Timm, A. Mouchet: Deconstructing the last glacial termination, Quaternary Science Reviews, in press; IPRC-756]

The role of CO_2 hydrates in deglacial climate change

A new hypothesis for the glacial-interglacial atmospheric CO_2 cycles was set forth that involves CO_2 storage and release from the margins of submarine volcanic systems in the Pacific Ocean. Recent on-site surveys indicate the CO_2 flux from submarine volcanoes in the Pacific is underestimated in global carbon budgets. These surveys have documented large accumulations of liquid CO_2 and CO_2-rich fluids in the sediments that blanket submarine volcanic arcs, but the total amount and spatial extent of these accumulations is not known. The flux of CO_2 from these accumulations is partly regulated by caps of CO_2 hydrate and CO_2-saturated pore waters at the sediment–water interface. Our hypothesis predicts that as the oceans cooled during glaciations, the zones of CO_2 hydrate stability expanded, thereby reducing the net flux of CO_2 from these sites to the ocean and atmosphere. During deglacial warming the hydrate zone deepened, releasing buoyant liquid CO_2 and CO_2-rich fluids that accumulated during the glacial. We show that the timing and magnitude of temperature change during the last deglaciation could account for a significant reduction in regional extent of CO_2 hydrate stability. This hypothesis would account for the large radiocarbon activity ($D^{14}C$) anomaly at intermediate water depths in the Pacific during the last deglaciation and the simultaneous 190‰ decline in atmospheric $D^{14}C$. This hypothesis also reconciles why deep-sea carbon isotope gradients in the deep Pacific did not change and why the $D^{14}C$ ages of deep waters were not anomalously old during the last glacial.

[L. Stott, A. Timmermann: Hypothesized Link between Glacial/Interglacial Atmospheric CO2 Cycles and Storage/Release of CO_2-Rich Fluids from the Deep Sea, AGU monograph series, in press]

Chapter 5: Developments at the Asia-Pacific Data Center (APDRC)

3.1 DATA SERVICES

The overarching goal of the APDRC data services is to provide easy access to the local and remote global climate data base and products, and to provide the required data management and metadata for easy usability of these data and products. This includes both the management of these data (DM) and the data server systems (DSS) used to serve these data. In the past, these two activities were kept separate, but as the APDRC continued to evolve, they have become more tightly integrated.

The APDRC/JAMSTEC collaboration focuses on three main projects: data management and services, data support for JII research, and product development. This work is carried out in collaboration with the JAMSTEC data group, previously directed by Dr. Awaji. In March 2010, the two groups held a small workshop at the IPRC. During this meeting, plans for future collaborations were made. Dr. Awaji described the new JAMSTEC Data Research Center (DrC). It was decided that the best way forward would be for DrC to continue to develop with help from the APDRC, and the APDRC would continue to support IPRC/JAMSTEC researchers. DrC has a mission to archive all the JAMSTEC data (including physical specimens, e.g., cores), whereas the APDRC expertise is more specific to geophysical data. While the APDRC will continue to advise JAMSTEC on data-serving issues, the APDRC will focus on data services to all JII researchers.

Data-services support this past year has focused on transferring the complete hindcast output from OFES to the APDRC servers. A new dedicated server was purchased. The new machine was configured with a large RAID disk for storage. Other data sets were updated as needed, and a new data specialist (Michael Mehari) was hired to assist with these tasks.
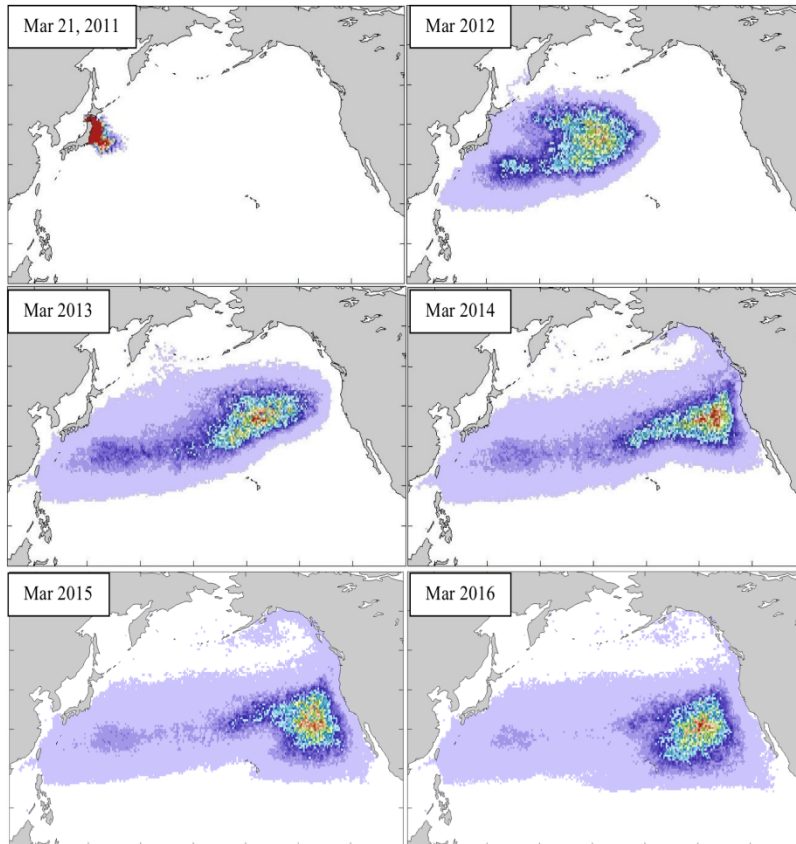
3.2 DATA PRODUCTS

Support to IPRC researchers, as well as recent data products, can be viewed on the APDRC projects page (http://apdrc.soest.hawaii.edu/projects). Highlights include on-going Argo-based data products, seasonal precipitation forecast for the Pacific [H. Annamalai and colleagues] and a high-wind events data set [T. Sampe and Shang-Ping Xie].

Surface CUrrents assessed from a Diagnostic model (SCUD) data set and applications

As noted in last year's report, a global high-resolution surface data set, called Surface CUrrents assessed from a Diagnostic model (SCUD), is being produced at IPRC and made available to the public via APDRC servers. In FY10 the global mean dynamic ocean topography was updated using the most recent satellite and in situ data. The product was used to study the dynamics of the Azores Current. An improved statistical model of observed motion of surface drifters and the diagnostic surface velocity product were used to investigate the open ocean and coastal areas that may collect floating marine debris. This study led to better understanding of structure and dynamics of marine debris in the North Atlantic (Law et al, 2010, IPRC-717) and what may be the first detection of microplastic in the subtropical South Atlantic and South Indian Ocean (in

collaboration with M. Eriksen, "5 Gyres/Algalita") and in the South Pacific (in collaboration with J. Mackey.).

After the tsunami of March 11, 2011, the probable pathways of the debris from Japan towards the east have been computed from the statistical model. The debris is predicted to reach Midway, the Hawaiian Islands, the US West Coast, and the area of the North Pacific Garbage Patch in 1, 2, 3, and 5 years, respectively.

Snapshots from the statistical model projections for the trajectory of the floating tsunami debris. Red indicates highest debris concentration, light purple, least.

Daily maps of the assessed location and distribution of the debris, derived using the SCUD model, are also made available to the public.

[L. Lamas, A. Peliz, I. Ambar, A. Barbosa Aguiar, N. Maximenko, and A.Teles-Machado, 2010: Evidence of time-mean cyclonic cell southwest of Iberian Peninsula: The Mediterranean Outflow-driven beta-plume? *Geophys. Res. Lett.*, **37**, L12606, doi:10.1029/2010GL043339. IPRC-698; N. Maximenko, J. Hafner, and P. Niiler: Pathways of marine debris from trajectories of Lagrangian drifters, submitted to *Marine Pollution Bulletin*].

PUBLICATIONS

Published Papers

Annamalai, H., S. Kida and J. Hafner, 2010: Potential impact of the tropical Indian Ocean - Indonesian Seas on El Nino characteristics. *J. Climate*, **23**, 3933–3952. IPRC-680.

Ascani, F., E. Firing, P. Dutrieux, J. P. McCreary, A. Ishida, 2010: Deep equatorial ocean circulation induced by a forced-dissipated Yanai beam. *J. Phys. Oceanogr.*, **40**, 1118-1142. IPRC-662.

Chen, J.-M., T. Li, C.-F. Shih, 2010: Tropical Cyclone– and Monsoon-Induced Rainfall Variability in Taiwan. *J. Climate*, **23**, 4107–4120. doi:10.1175/2010JCLI3355.1. IPRC-685.

Chen, J., T. Qu, Y. N. Sasaki, and N. Schneider, 2010: Anti-correlated variability in subduction rate of the western and eastern North Pacific Oceans identified by an eddy-resolving ocean GCM. *Geophys. Res. Lett.*, **37**, L23608, doi:10.1029/2010GL045239. IPRC-733.

Chowdary, J. S., S.-P. Xie, J.-J. Luo, J. Hafner, S. Behera, Y. Masumoto, and T. Yamagata, 2011: Predictability of Northwest Pacific climate during summer and the role of the tropical Indian Ocean. *Clim. Dyn.*, **36** (607), 621, IPRC-640.

Chowdary, J. S., S.-P. Xie, J.-Y. Lee, Y. Kosaka, and B. Wang, 2010: Predictability of summer Northwest Pacific climate in 11 coupled model hindcasts: Local and remote forcing. *J. Geophys. Res.-Atmos.*, **115**, D22121, doi:10.1029/2010JD014595. IPRC-716.

Christie, M. R., B. N. Tissot, M. A. Albins, J. P. Beets, Y.Jia, D. M. Ortiz, S. E. Thompson, and M. A. Hixon, 2010: Larval Connectivity in an Effective Network of Marine Protected Areas. *Plos ONE*, **5** (12), e15715, IPRC-748.

Dohan, K., and N. Maximenko, 2010: Monitoring ocean currents with satellite sensors. *Oceanography*, **23** (4), 94-103. IPRC-749.

Du, Y., and T. Qu, 2010: Three inflow pathways of the Indonesian throughflow as seen from the Simple Ocean Data Assimilation. *Dyn. of Atmos. and Oceans*, **50** (2), 233–256. IPRC-687.

Elison Timm, O., H. F. Diaz, T .W. Giambelluca, M. Takahashi, 2011: Projection of Changes in the Frequency of Heavy Rain Events over Hawaii Based on Leading Pacific Climate Modes. *J. Geophys. Res.-Atmos.*, **116**, D041. IPRC-744.

Fudeyasu, H., Y. Wang, M. Satoh, T. Nasuno, H. Miura, W. Yanase, 2010: Multiscale Interactions in the Lifecycle of a Tropical Cyclone Simulated in a Global Cloud-System-Resolving Model: Part I: Large-scale and Storm-scale Evolutions. *Mon. Wea. Rev.*, **138**, 4285–4304, doi: 10.1175/2010MWR3474.1. IPRC-713.

Fudeyasu, H., Y. Wang, M. Satoh, T. Nasuno, H. Miura, W. Yanase, 2010: Multiscale Interactions in the Lifecycle of a Tropical Cyclone Simulated in a Global Cloud-System-Resolving Model: Part II: System-Scale and Mesoscale Processes. *Mon. Wea. Rev.*, **138**, 4305–4327.doi: 10.1175/2010MWR3475.1. IPRC-714.

Gao, S., T. Qu, I. Fukumori, 2011: Effects of mixing on the subduction of South Pacific waters identified by a simulated passive tracer and its adjoint. *Dyn. Atmos. and Oceans*, **51**, 45-54. IPRC-738.

Gu, D.-J., T. Li, Z.-P. Ji, and B. Zheng, 2010: Connection of the South China Sea summer monsoon to maritime continent convection and ENSO. *J. of Trop. Meteor.*, **16**, 10.3969/j.issn.1006-8775.2010.01.001. IPRC-654.

Gu, D., T. Li, Z. Ji, B. Zheng, 2010: On the Phase Relations between the Western North Pacific, Indian, and Australian Monsoons. *J. Climate*, **23**, 5572–5589. doi: 10.1175/2010JCLI2761.1. IPRC-682.

Heinemann, M., A.Timmermann, and U. Feudel, 2011: Interactions between marine biota and ENSO: A conceptual model analysis. *Nonlin. Processes Geophys.*,**18**, 29-40. IPRC-747.

Hendricks, E.A., M. S. Peng, B. Fu, and T. Li, 2010: Quantifying environmental control on tropical cyclone intensity change. *Mon. Wea. Rev.*, **138**, 3243-3271. IPRC-758.

Hong, C.-C., and T. Li, 2010: The independence of SST skewness from thermocline feedback in the eastern equatorial Indian Ocean. *Geophys. Res. Lett.*, **37**, L11702, doi:10.1029/2010GL043380. IPRC-692.

Hong, C.-C., T. Li, H. Lin, and Y.-C. Chen, 2010: Asymmetry of the Indian Ocean Basinwide SST Anomalies: Roles of ENSO and IOD. *J. Climate*, **23**, 3563–3576. doi: 10.1175/2010JCLI3320.1. IPRC-674.

Hsin, Y.-C., T. Qu, and C.-R. Wu, 2010: Intra-seasonal variation of the Kuroshio southeast of Taiwan and its possible forcing mechanism. *Ocean Dynamics*, **60** (5), 1293–1306. IPRC-690.

Hsu, P.-C., and T. Li, 2011: Interactions between boreal summer Intraseasonal oscillations and synoptic-scale disturbances over the western North Pacific. Part II: Apparent heat and moisture sources and eddy momentum transport. *J. Climate*, **24** (3), 942-961IPRC-723.

Hsu, P.-C., T. Li, and C.-H. Tsou, 2011: Interactions between boreal summer Intraseasonal oscillations and synoptic-scale disturbances over the western North Pacific. Part I: Energetics diagnosis. *J. Climate*, **24**(3), 927-941 IPRC-722.

Huang, G., K. Hu, and S.-P. Xie, 2010: Strengthening of tropical Indian Ocean teleconnection to the Northwest Pacific since the mid-1970s: An atmospheric GCM study. *J. Climate*, **23**, 5294–5304. doi: 10.1175/2010JCLI3577.1IPRC-704.

Johnson, N. C., and S.-P. Xie, 2010: Changes in the sea surface temperature threshold for tropical convection *Nature Geoscience*, **3** (12), 842-845. IPRC-751.

Kawatani,Y., K. Hamilton, and S. Watanabe, 2011: The quasi-biennial oscillation in a double CO2 climate. *J. Atmos. Sci.*, **68**, 265-283, IPRC-737.

Kikuchi, K., and B. Wang, 2010: Formation of tropical cyclones in the northern Indian Ocean associated with two types of tropical intraseasonal oscillation modes. *J. Meteor. Soc. Japan*, **88** (3), 475–496. IPRC-657.

Kikuchi, K., and B. Wang, 2010: Spatio-temporal wavelet transform and the multiscale behavior of the Madden-Julian Oscillation. *J. Climate*, **23** (14), 3814–3834. IPRC-664.

Kug, J.-S., K.P. Sooraj, T. Li, F.-F. Jin, and I.-S. Kang, 2010: Precursors of the El Niño/La Niña onset and their inter-relationship. *J. Geophys. Res.*, **115**, D05106, doi:10.1029/2009JD012861. IPRC-757.

Kuwano-Yoshida, A., S. Minobe, S.-P. Xie, 2010: Precipitation Response to the Gulf Stream in an Atmospheric GCM. *J. Climate*, **23**, 3676–3698, doi: 10.1175/2010JCLI3261.1. IPRC-689.

Lamas, L., A. Peliz, I. Ambar, A. Barbosa Aguiar, N. Maximenko, and A.Teles-Machado, 2010: Evidence of time-mean cyclonic cell southwest of Iberian Peninsula: The Mediterranean Outflow-driven beta-plume? *Geophys. Res. Lett.*, **37**, L12606, doi:10.1029/2010GL043339. IPRC-698.

Lauer, A., K. Hamilton, Y. Wang, V.T.J. Phillips, and R. Bennartz, 2010: The Impact of Global Warming on Marine Boundary Layer Clouds over the Eastern Pacific - A Regional Model Study. *J. Climate*, **23** (21), 5844–5863. IPRC-706.

Law, K.L., S. Morét-Ferguson, N.A. Maximenko, G. Proskurowski, E.E. Peacock, J. Hafner, and C.M. Reddy, 2010: Plastic accumulation in the North Atlantic Subtropical Gyre. *Science*, **329**, 1185–1188. IPRC-717.

Lee, J.-Y., et al., 2010: How are seasonal prediction skills related to models' performance on mean state and annual cycle? *Clim. Dyn.*, **35**, 267–283. IPRC-703.

Lee, S.-S., J.-Y. Lee, K.-J. Ha, B. Wang, J. Kyung, and E. Schemm, 2011: Deficiencies and possibilities for long-lead coupled climate prediction of the western North Pacific-East Asian summer monsoon. *Clim. Dyn.*, **36** (5), 1173-1188. IPRC-697.

Li, C., T. Li, J. Liang, D. Gu, A. Lin, and B. Zheng, 2010: Interdecadal variations of meridional winds in the South China Sea and their relationship with summer climate in China. *J. Climate*, **23**, 825–841. IPRC-661.

Li, T., M. Kwon, M. Zhao, J.-S. Kug, J.-J. Luo, and W. Yu, Global warming shifts Pacific tropical cyclone location. *Geophys. Res. Lett.*, **37**, doi:10.1029/2010GL045124. IPRC-720.

Martinez, E., and K. J. Richards: Impact of spatio-temporal heterogeneities and lateral stirring and mixing on midwater biotic interactions. *J. Mar. Sys.*, **82** (3), 122-134. IPRC-688.

Matsumura, S., G. Huang, S.-P. Xie, and K. Yamazaki, 2010: SST-forced and internal variability of the atmosphere in an ensemble GCM simulation. *J. Meteor. Soc. Japan*, **88**, 43–62. IPRC-659.

Melnichenko, O.V., N.A. Maximenko, N. Schneider, and H. Sasaki, 2010: Quasi-stationary striations in basin-scale oceanic circulation: Vorticity balance from observations and eddy-resolving model. *Ocean Dynamics*, **60** (3), 653–666. IPRC-666.

Minobe, S., M. Miyashita, A. Kuwano-Yoshida, H. Tokinaga, and S.-P. Xie, 2010: Atmospheric response to the Gulf Stream: Seasonal variations. *J. Climate*, **23**, 3699–3719. IPRC-671.

Murakami, H., and B. Wang, 2010: Future Change of North Atlantic Tropical Cyclone Tracks: Projection by a 20-km-Mesh Global Atmospheric Model. *J. Climate*, **23**, 2699–2721. IPRC-679.

Nagano, A., K. Ichikawa, H. Ichikawa, H. Tomita, H. Tokinaga, and M. Konda, 2010: Stable volume and heat transports of the North Pacific subtropical gyre revealed by indentifying the Kuroshio in synoptic hydrography south of Japan. *J. Geophys. Res.-Oceans*, **115**, C09002, doi:10.1029/2009JC00574. IPRC-694.

Nakamura, M., M. Kadota, and S. Yamane, 2010: Quasi-geostrophic transient wave activity flux: Updated climatology and its role in polar vortex anomalies. *J. Atmos Sci.*, **67**, 3164–3189. IPRC-725.

Okazaki, Y., A. Timmermann, L. Menviel, N. Harada, A. Abe-Ouchi, M.O. Chikamoto, A. Mouchet, and H. Asahi, 2010: Deep Water Formation in the North Pacific During the Last Glacial Termination. *Science*, **329** (5988), 200–204. IPRC-707.

Qu, T., S. Gao, I. Fukumori, R.A. Fine, and E.J. Lindstrom, 2010: The obduction of Equatorial 13°C Water in the Pacific identified by a simulated passive tracer. *J. Phys. Oceanogr.*, **40** (10), 2282–2297. IPRC-699.

Richter, I., and S.-P. Xie, 2010: Moisture transport from the Atlantic to the Pacific basin and its response to North Atlantic cooling and global warming. *Clim. Dyn.*, **35**, 551–566, DOI: 10.1007/s00382-009-0708-3. IPRC-660.

Sampe, T., H. Nakamura, A. Goto, and W. Ohfuchi, 2010: Significance of a midlatitude SST frontal zone in the formation of a storm track and an eddy-driven westerly jet. *J. Climate*, **23** (7), 1793–1814. IPRC-656.

Sasaki, H., S.-P. Xie, B. Taguchi, M. Nonaka, and Y. Masumoto, 2010: Seasonal variations of the Hawaiian Lee Countercurrent induced by the meridional migration of the trade winds. *Ocean Dynamics*, **60**, 705–715, DOI: 10.1007/s10236-009-0258-6. IPRC-639.

Shankar, D., S.G. Aparna, J.P. McCreary, I. Suresh, S. Neetu, F. Durand, S.S.C. Shenoi, and M.A. Al Saafan, 2010: Minima of interannual sea-level variability in the Indian Ocean. *Progr. in Oceanograph*y, **84**, 225–241. IPRC-636.

Stein, K., N. Schneider, A. Timmermann, and F.-F. Jin, 2010: Seasonal synchronization of ENSO events in a linear stochastic model. *J. Climate*, **23**, 5629–5643.
doi: 10.1175/2010JCLI3292.1. IPRC-702.

Su, J., R. Zhang, T. Li, X. Rong, J. Kug, and C.-C. Hong, 2010: Amplitude asymmetry of El Nino and La Nina in the eastern equatorial Pacific, *J. Climate*, **23**, 605-617. IPRC-761.

Taguchi, B., B. Qiu, M. Nonaka, H. Sasaki, N. Schneider, S.-P. Xie, 2010: Decadal variability of the Kuroshio Extension: Mesoscale eddies and recirculations. *Ocean Dynamics*, **60** (3), 673-691. IPRC-691.

Tanimoto, Y., T. Kajitani, H. Okajima, and S.-P. Xie, 2010: A peculiar feature of the seasonal migration of the South American rain band. *J. Meteor. Soc. Japan*, **88**, 79-90. IPRC-655.

Timm, O., P. Koehler, A. Timmermann, and L. Menviel, 2010: Mechanisms for the onset of the African Humid Period and Sahara Greening 14.5–11 ka BP. *J. Climate*, **23**, 2612–2633. doi: 10.1175/2010JCLI3217.1. IPRC-642.

Timmermann, A., J. Knies, O. Elison Timm, A. Abe-Ouchi, and T. Friedrich, 2010: Promotion of glacial ice-sheet buildup 60-115 kyr B.P. by precessionally paced Northern Hemispheric meltwater pulses. *Paleoceanography*, **25**, PA4208, doi:10.129/2010PA001933. IPRC-708.

Timmermann, A., S. McGregor, and F.-F. Jin, 2010: Wind effects on past and future regional sea-level trends in the southern Indo-Pacific. *J. Climate*, **23**, 4429–4437, doi: 10.1175/2010JCLI3519.1. IPRC-686.

Tokinaga, H., S.-P. Xie, 2011: Weakening of the equatorial Atlantic cold tongue over the past six decades. *Nature Geoscience*, doi:10.1038/ngeo1078,. IPRC-753.

Tokinaga, T., and S.-P. Xie, 2011: Wave and Anemometer-based Sea-surface Wind (WASWind) for climate change analysis. *J. Climate*, **24**, 267-285. IPRC-718.

Wang, B., Y. Yang, Q.-H. Ding , H. Murakami, and F. Huang, 2010: Climate Control of Global Tropical Storm Days (1965-2008): El Niño and Global Warming. *Geophys. Res. Lett.*, **37**, L07704, doi:10.1029/2010GL042487. IPRC-673.

Wang, Y., and J. Xu, 2010: Energy production, frictional dissipation, and maximum intensity of a numerically simulated tropical cyclone. *J. Atmos. Sci.,* **67**, 97-116. IPRC-621.

Wen, M., T. Li, R. Zhang, and Y. Qi, 2010: Structure and origin of the quasi-biweekly oscillation over the tropical Indian Ocean in boreal spring. *J. Atmos. Sci.,* **67,** 1965-1982. IPRC-760.

Wu, B., T. Li, T. Zhou, 2010: Asymmetry of Atmospheric Circulation Anomalies over the Western North Pacific between El Niño and La Niña. *J. Climate*, **23**, 4807–4822.
doi: 10.1175/2010JCLI3222.1. IPRC-683.

Wu, B., T. Li, T. Zhou, 2010: Relative Contributions of the Indian Ocean and Local SST Anomalies to the Maintenance of the Western North Pacific Anomalous Anticyclone during the El Niño Decaying Summer. *J. Climate*, **23**, 2974–2986. doi: 10.1175/2010JCLI3300.1. IPRC-684.

Xie, B.-G., Q.-H. Zhang, and Y. Wang, 2010: Observed characteristics of hail size in four regions in China during 1980-2005. *J. Climate*, **23**, 4973-4982, doi: 10.1175/2010JCLI3600.1. IPRC-700.

Xie, S.-P., Y. Du, G. Huang, X.-T. Zheng, H. Tokinaga, K. Hu, Q. Liu, 2010: Decadal Shift in El Niño Influences on Indo–Western Pacific and East Asian Climate in the 1970s. *J. Climate*, **23**, 3352–3368. doi: 10.1175/2010JCLI3429.1. IPRC-669.

Xu, H., H. Tokinaga, and S.-P. Xie, 2010: Atmospheric Effects of the Kuroshio Large Meander during 2004-05. *J. Climate*, **23**, 4704–4715. IPRC-695.

Xu, J., and Y. Wang ,2010: Sensitivity of tropical cyclone inner core size and intensity to the radial distribution of surface entropy flux. *J. Atmos. Sci.*, **67** (6), 1831-1852. IPRC-667.

Xu, J., Y. Wang, 2010: Sensitivity of the Simulated Tropical Cyclone Inner-Core Size to the Initial Vortex Size. *Mon. Wea. Rev.*, **138**, 4135–4157. doi: 10.1175/2010MWR3335.1. IPRC-705.

Yoshida, S., B. Qiu, and P. Hacker, 2010: Wind-generated eddy characteristics in the lee of the island of Hawaii. *J. Geophys. Res.-Oceans*, **115**, C03019, doi:10.1029/2009JC005417. IPRC-651.

Zhan, R., Y. Wang, and X. Le, 2011: Contributions of ENSO and East Indian Ocean SSTA to the Interannual Variability of Tropical Cyclone Frequency. *J. Climate*, **24**,509-521, doi: 10.1175/2010JCLI3808.1. IPRC-721.

Zhou, C., T. Li, 2010: Upscale Feedback of Tropical Synoptic Variability to Intraseasonal Oscillations through the Nonlinear Rectification of the Surface Latent Heat Flux. *J. Climate*, **23**, 5738–5754. doi: 10.1175/2010JCLI3468.1. IPRC-693.

Zhu, W., T. Li, X. Fu, and J.-J. Luo: Influence of the Maritime Continent on the boreal summer intraseasonal oscillation. *J. Meteor. Soc. Japan*, **88**, 395-407. IPRC-681.

Zhuang, W., S.-P. Xie, D. Wang, B. Taguchi, H. Aiki, and H. Sasaki, 2010: Intraseasonal variability in sea surface height over the South China Sea. *J. Geophys. Res.-Oceans*, **115**, C04010, doi:10.1029/2009JC005647. IPRC-658.

In press

For up-to-date listing of publications see our website http://iprc.soest.hawaii.edu/publications/sci_articles.php

Ajayamohan, R. S., H. Annamalai, J.-J. Luo, J. Hafner and T. Yamagata: Poleward Propagation of Boreal Summer Intraseasonal Oscillations in a Coupled Model: Role of Internal Processes. *Clim. Dyn.*, IPRC-696.

Chelton, D.B., and S.-P. Xie: Coupled ocean-atmosphere interaction at oceanic mesoscales. *Oceanography*, IPRC-719.

Chung, P.-H., C.-H. Sui, and T. Li: Interannual relationships between the tropical SST and summertime subtropical anticyclone over the western North Pacific. *Journal of Geophysical Research*, IPRC-773.

Ding, Q., B. Wang, J. M. Wallace, and G. Branstator: Tropical-extratropical teleconnections in boreal summer: Observed interannual variability. *J. Climate*, IPRC-745.

Du, Y., L. Yang, and S.-P. Xie: Tropical Indian Ocean influence on Northwest Pacific tropical cyclones in summer following strong El Nino. *J. Climate*, IPRC-730.

Friedrich, T., A. Timmermann, L. Menviel, O. Elison Timm, A. Mouchet, D. M. Roche: The mechanism behind internally generated centennial-to-millennial scale climate variability in an earth system model of intermediate complexity. *Geoscientific Model Development*,**116**, D04109. IPRC-710.

Fudeyasu, H., and Y. Wang: Balanced contribution to the intensification of a tropical cyclone simulated in TCM4: Outer core spin-up process, *J. Atmos. Sci.*, IPRC-741.

Gao, J.-Y., and T. Li: Factors controlling multiple tropical cyclone events in the western North Pacific. *Mon. Wea. Rev.*, IPRC-729.

Hsu, P.-c., T. Li, and B. Wang: Trends in Global Monsoon area and precipitation over the past 30 years. *Geophys. Res. Lett.*, IPRC-754.

Jayakumar, A., J. Vialard, M. Lengaigne, C. Gnanaseelan, J.P. McCreary, B. Praveen Kumar: Processes controlling the surface temperature signature of the Madden-Julian Oscillation in the thermocline ridge of the Indian Ocean. *Clim. Dyn.*, IPRC-739.

Kilpatrick, T., N. Schneider, E. Di Lorenzo: Generation of low-frequency spiciness variability in the thermocline. *J. Phys. Oceanogr.*, IPRC-726.

Kosaka,Y., S.-P. Xie, and H. Nakamura: Dynamics of interannual variability in summer precipitation over East Asia. *J. Climate*, IPRC-771.

Kosaka,Y.: The Silk Road pattern revisited, *Tenki (Bull. Meteor. Soc. Japan)*, IPRC-772.

Lee, S.-S., J.-Y. Lee, B. Wang, F.-F. Jin, W.-J. Lee, and K.-J. Ha: A comparison of climatological subseasonal variations in the wintertime storm track activity between the North Pacific and Atlantic: Local energetics and moisture effect. *Clim. Dyn.*, IPRC-750.

Lee, J.-Y., B. Wang, Q. Ding, K.-J. Ha, J.-B. Ahn, A. Kumar, B. Stern, and O. Alves: How predictable is the Northern Hemisphere summer upper-tropospheric circulation? *Clim. Dyn.*, IPRC-622.

Lee, S., T. Gong, N. Johnson, S. Feldstein, D. Pollard: On the possible link between tropical convection and the Northern Hemisphere Arctic surface air temperature change between 1958-2001. *J. Climate*, IPRC-768.

Li, J., S.-P. Xie, E. R. Cook, G. Huang, R. D. Arrigo, F. Liu, J. Ma, X.-T. Zheng : Interdecadal modulation of El Niño amplitude during the past millennium. Nature Climate Change, IPRC-774.

Lin, A.-L., T. Li, X. Fu, J.-J. Luo, and Y. Masumoto: Effects of air-sea coupling on the boreal summer intraseasonal oscillations over the Tropical Indian Ocean. *Clim. Dyn.*, IPRC-736.

Liu, L., W. Yu, and T. Li, 2011: Dynamic and Thermodynamic Air-Sea Coupling Associated with the Indian Ocean Dipole diagnosed from 23 WCRP CMIP3 Models. *J. Climate*, IPRC-769.

McGregor, S., and A. Timmermann: The effect of explosive tropical volcanism on ENSO. *J. Climate*, IPRC-740.

McLeod, E., R. Moffitt, A. Timmermann, R. Salm, L. Menviel, M. Palmer, E. Selig, K.S. Casey, J. Bruno: Warming Seas in the Coral Triangle: Coral Reef Vulnerability and Management Implications. *Coastal Management*, IPRC-712.

Menviel, L., A. Timmermann, O. Elison Timm, A. Mouchet, A. Abe-Ouchi, M.O. Chikamoto, N. Harada, R. Ohgaito and Y. Okazaki: Removing the North Pacific halocline: Effects on global climate, ocean circulation and the carbon cycle. *Deep Sea Res. II*, IPRC-724.

Menviel, L., A. Timmermann, O. Elison Timm, A. Mouchet: Climate and biogeochemical response to a rapid melting of the West-Antarctic Ice Sheet during interglacials and implications for future climate. *Paleoceanography*, IPRC-734.

Menviel, L., A. Timmermann, O. Elison Timm, A. Mouchet: Deconstructing the Last Glacial Termination: the role of millennial and orbital-scale forcings. *Quaternary Science Reviews*, IPRC-756.

Moon, J.-Y., B. Wang, K.-J. Ha: ENSO regulation of MJO teleconnection. *Clim. Dyn.*, IPRC-715.

Murakami, H., B. Wang, and A. Kitoh: Future change of western North Pacific typhoons: Projections by a 20-km-mesh global atmospheric model. *J. Climate*, IPRC-727.

Qu, T., S. Gao, and I. Fukumori: What governs the North Atlantic salinity maximum in a global GCM? *Geophys. Res. Lett.*, IPRC-763.

Richter, I., S.-P. Xie, A. T. Wittenberg, Y. Masumoto: Tropical Atlantic biases and their relation to surface wind stress and terrestrial precipitation. *Climate Dynamics*, IPRC-765.

Righi, M., C. Klinger, V. Eyring, J. Hendricks, A. Lauer, A. Petzold: The climate impact of biofuels in shipping: global model studies of the aerosol indirect effect. *Environmental Science & Technology*, IPRC-752.

Sasaki, Y., and N. Schneider: Decadal shifts of the Kuroshio Extension jet: Application of thin-jet theory. *J. Phys. Oceanogr.*, IPRC-746.

Seo, H. and S.-P. Xie: Response and impact of equatorial ocean dynamics and tropical instability waves in the tropical Atlantic under global warming: A regional coupled downscaling study. *J. Geophys. Res.-Oceans*, IPRC-762.

Small III, A. A., J. B. Stefik, J. Verlinde, N. C. Johnson: The Cloud Hunter's Problem: An Automated Decision Algorithm to Improve the Productivity of Scientific Data Collection in Stochastic Environments. *Mon. Wea. Rev.*, IPRC-755.

Song, Y. T., and T. Qu : Multiple Satellite Missions Confirming the Theory of Seasonal Oceanic Variability in the northern North Pacific. *Marine Geodesy*, IPRC-766.

Tanimoto, Y., T. Kanenari, H.Tokinaga, S.-P. Xie: Sea level pressure minimum along the Kuroshio and its extension. *J. Climate*, IPRC-764.

Thompson, A.F., P. H Haynes, Chris Wilson, and K. J. Richards: Rapid Southern Ocean front transitions in an eddy-resolving ocean GCM. *Geophys. Res. Lett.*, IPRC-732.

Uchikawa, J., B. N. Popp, J. E. Schoonmaker, A. Timmermann, S. J. Lorenz: Geochemical and climate modeling evidence for Holocene aridification in Hawaii: Dynamic response to a weakening equatorial cold tongue, *Quaternary Science Reviews*, IPRC-711.

Wang, B., H.-J. Kim, K. Kikuchi, and A. Kitoh: Diagnostic metrics for evaluation of annual and diurnal cycles. *Clim. Dyn.*, IPRC-709.

Wyant, M.C., et al.: The PreVOCA experiment: Modeling the lower troposphere in the Southeast Pacific. *Atmospheric Chemistry and Physics*, PRC-701.

Xiang, B., W. Yu, T. Li, and B. Wang: The critical role of the boreal summer mean state in the development of the IOD, *Geophys. Res. Lett.*. IPRC-742.

Xie, S.-P., L.-X. Xu, Q. Liu, and F. Kobashi: Dynamical role of mode-water ventilation in decadal variability in the central subtropical gyre of the North Pacific. *J. Climate*, IPRC-728.

Yim, S.-Y., J.-G. Jhun, R. Lu, and B. Wang: Two distinct patterns of spring Eurasian snow cover anomaly and their impacts on the East Asian summer monsoon. *J. Geophys. Res.-Atmos.*, IPRC-731.

Zhang, S., J.W. Liu, S.-P. Xie, and X. Meng: The formation of a surface anticyclone in the spring Yellow and East China Seas. *J. Meteor. Soc. Japan*, IPRC-770.

Zhou, X., and B. Wang: Mechanism of Concentric Eyewall Replacement Cycles and Associated Intensity Change. *J. Atmos. Sci.*, IPRC-743.

Zhou, Xi., B. Wang, X. Ge, T.Lli: Impact of secondary eyewall heating on tropical cyclone intensity change. *J. Atmos. Sci*., IPRC-735.

Book

Nagothu, U. S., B. Geethalakshmi, H. Annamalai, A. Lakshmanan, 2011: *Sustainable rice production on a warmer planet: Linking science, stakeholders and policy*. New Delhi, Macmillan Publ. India, Ltd. , IPRC-767.

Technical Note

Maximenko, N. A., and J. Hafner, 2010: SCUD: Surface CUrrents from Diagnostic model, IPRC Tech. Note 5, 17pp.

THE YEAR'S WORKSHOPS AND CONFERENCES

DATE	TITLE
March 20, 2011	Hydrodynamics of Marine Debris (Program) Workshop at the 5th International Marine Debris Conference
February 28 – March 4, 2011	The AGU Chapman Conference: "Atmospheric Gravity Waves and Their Effects on General Circulation and Climate"
January 19 – 20, 2011	SOEST Symposium: "The Science of Climate Change in Hawaii"
December 21, 2010	Workshop: Air-sea Interaction and Climate Variability over the Northwest
November 4 – 5, 2010	3rd OFES International Workshop in Japan
August 18, 2010	Mini-Workshop: Multi-scale Circulation Variability in the Tropical Western Pacific Ocean
August 2, 2010	Mini-symposium: Ocean Salinity and the Global Water Cycle
May 27, 2010	Tenth Annual IPRC Symposium
April 21, 2010	Mini-symposium: Clouds, Chemistry, and Climate

The Year's Seminars

Date	Speaker	Affiliation	Title
March 31, 2011	Randall J. Alliss	Northrop Grumman Corporation	*Maximizing and Optimizing the Large Scale Deployment and Integration of Renewable Energy*
*March 18, 2011	Pallav Ray	IPRC	*On the Initiation of the Madden-Julian Oscillation (MJO)*
March 16, 2011	Hidekatsu Yamazaki	Tokyo University of Marine Science and Technology, Tokyo, Japan	*The Kuroshio and Mixing Phenomena*
March 7, 2011	Fuqing Zhang	Penn State University	*Prediction, Predictability and Data Assimilation of Tropical Cyclones*
**March 3, 2011	François Ascani	IPRC	*The role of dissipation in wave-induced transport in a basin*
**Feb. 10, 2011	Ali Bel Madani	IPRC	*Intraseasonal Kelvin Waves and Humboldt Current Eddies*
*February 9, 2011	Bunmei Taguchi	JAMSTEC	*Seasonal evolutions of atmospheric response to decadal SST anomalies in the North Pacific subarctic frontal zone*
*January 26, 2011	Kevin Hamilton	IPRC	*Equilibrium Climate Sensitivity*
**January 20, 2011	Zuojun Yu	IPRC	*Oxygen Minimum Zones in the Northern Indian Ocean*
January 18, 2011	Sarah Kang	Columbia University, New York, New York	*The tropical response to extratropical thermal forcing: Theory and application*
**January 13, 2011	Malte Heinemann	IPRC	*Warm and Sensitive Paleocene-Eocene Climate*
December 17, 2010	Jerry Meehl	National Center for Atmospheric Research, Boulder Colorado	*Decadal Variability of Asian-Australian Monsoon-ENSO-TBO Relationships*
**Thursday, December 2, 2010	Niklas Schneider	IPRC	*Rotating Table*
*Wednesday, December 1, 2010	Nat Johnson	IPRC	*Changes in the sea surface temperature threshold for tropical convection*

Date	Speaker	Affiliation	Title
November 18, 2010	Carsten Eden	Centre for Marine and Atmospheric Sciences, Hamburg, Germany	*A dynamically consistent closure for zonally averaged ocean models*
*Nov. 17, 2010	Oliver Elison Timm	IPRC	*Statistical downscaling of future rainfall changes in Hawaii based on IPCC AR4 scenario simulations*
Nov. 9, 2010 IPRC 2010 Public Lecture in Climate Science	Susan Avery	Woods Hole Oceanographic Institution, Woods Hole, Massachusetts	*A Changing World, A Changing Ocean*
**Oct. 28, 2010	Neven Stjepan Fučkar	IPRC	*Adaptive scaling model of the main pycnocline and the associated overturning circulation*
*Oct. 27, 2010	Kevin Hamilton	IPRC	*The Brewer-Dobson Circulation Saga - From Crazy German Balloonists to the Future of the Global Climate*
*Oct. 20, 2010	Kazuhiro Oshima	Hokkaido University, Sapporo, Japan	*Response of North Pacific climate to global warming based on CMIP3 multi-model projections*
*Oct. 13, 2010	H. Annamalai	IPRC	*Moist static energy budget diagnostics for monsoon research*
*Oct. 6, 2010	Shang-Ping Xie	IPRC	*Indian Ocean capacitor effect on Northwest Pacific/East Asian climate: Dynamics and decadal change*
*Sept. 22, 2010	Yukiko Imada	University of Tokyo, Tokyo, Japan	*Climatic impact of tropical instability waves in the Pacific*
**Sept. 16, 2010	Oleg Melnichenko	IPRC	*Stationary Alternating Quasi-Zonal Jet-Like Structures in the Ocean*
**Sept. 2, 2010	Eitarou Oka	University of Tokyo, Tokyo, Japan	*New Aspects on the Formation and Circulation of the North Pacific Mode Waters Based on Profiling Float and Shipboard Measurements*
*Sept. 1, 2010	Tomohiko Tomita	Kumamoto University, Kumamoto, Japan	*Interannual Variability in the Baiu Front*
**Aug. 26, 2010	Meghan Cronin,	NOAA Pacific Marine Environmental Laboratory	*A Generalized Ekman Model for Frontal Regions*

Date	Speaker	Affiliation	Title
Aug. 19, 2010	Takatoshi Sakazaki	Hokkaido University, Sapporo, Japan	*Diurnal variations in the troposphere and stratosphere* cycle
Aug. 2, 2010	Gary Lagerloef	Earth & Space Research, Seattle, Washington	*The Aquarius salinity satellite mission and studies of the marine freshwater* cycle
July 8, 2010	Jessica Benthuysen	MIT/ WHOI Joint Program, Cambridge, Massachusetts	*Upwelling at a shelf break caused by buoyancy shutdown*
May 28, 2010	Matthew Widlansky	IPRC	*A general theory for the spatial and transient behavior of the South Pacific Convergence Zone*
**April 29th, 2010	James Potemra	IPRC	*The Hawaii Ocean Observing System*
***April 28, 2010	Richard Murnane	Risk Prediction Initiative Bermuda Institute for Ocean Sciences , St. George,Bermuda	*Natural Hazards and the Catastrophe Reinsurance Industry*
April 28, 2010	Stephan Lorenz	Max Planck Institute for Meteorology, Hamburg, Germany	*Climate impact of volcanic eruptions in ensemble simulations of the last millennium using the COSMOS model*
* April 21, 2010	June-Yi Lee	IPRC	*Predictable Mode Analysis on Seasonal Climate Anomalies*
****Monday, April 12, 2010	Dave Mattey	University of London, London, United Kingdom	*Fidelity of climate recording by modern and ancient stalagmites: Insight from cave monitoring in Gibraltar*

*   Joint IPRC-Meteorology Seminar

**   Joint IPRC-Oceanography Seminar

*** Special Seminar sponsored by the International Pacific Research Center, the University of Hawai'i Shidler College of Business MFE Program, the International Center for Climate and Society, and the University of Hawai'i Meteorology Department

**** Joint IPRC-G&G special seminar

LUNCHTIME DISCUSSIONS

DATE	SPEAKER	AFFILIATION	TITLE
March 14, 2011	Edward Cook	Tree-Ring Laboratory, Lamont-Doherty Earth Observatory, New York, New York	*Reconstructing the PDO from Long Tree-Ring Records: A Riddle Wrapped in a Mystery inside an Enigma*
March 8, 2011	Ryan L. Sriver	The Pennsylvania State University, University Park, Pennsylvania	Analyzing climate dynamics across time scales using mechanisms to link the past and possible futures
March 2, 2011	Takeshi Horinouchi	Hokkaido University, Sapporo, Japan	*Moist Hadley circulation: Constraints and the role of wave-convection coupling in an aqua-planet AGCM*
Feb. 1, 2011	Brad Murphy	Australian Bureau of Meteorology, Melbourne Australia	*The Pacific Climate Change Science Program: Improving understanding of climate science for Pacific nations*
Dec. 10, 2010	Ailie Gallant	University of Melbourne, Melbourne, Australia	*A 206-year multi-proxy rainfall reconstruction for south-eastern Australia*
Dec. 6, 2010	Paul J. Durack	CSIRO, Hobart, Australia	*Fifty years of water cycle change expressed in ocean salinity*
Nov. 19, 2010	Tanja Mildner	Centre for Marine and Atmospheric Sciences, Hamburg, Germany	*Impact of Last Glacial Maximum sea-level and surface-forcing changes on heat and freshwater transports in the Gulf of Mexico in an eddy-permitting ocean model*
Sep. 28, 2010	Nikolai Maximenko, Oleg Melnichenko, Jan Hafner, and Jeremy Soares	IPRC	*Accumulation of plastic debris on Kamilo Beach*
Sept. 24, 2010	Ali Bel Madani	IPRC	*ENSO feedbacks and time scale in a multimodel ensemble*
Aug. 31, 2010	Miho Ishizu	IPRC	*The oxygen-nitrate relationship of water mass in the Kuroshio Extension, Oyashio, and mixed water regions*

DATE	SPEAKER	AFFILIATION	TITLE
Aug. 27, 2010	Konstantin Lebedev	IPRC	*New gridded Argo products developed at the APDRC*
July 23, 2010	Rick Lumpkin	NOAA Atlantic Oceanographic and Meteorological Laboratory	*Surface Drifter Pair Spreading in the North Atlantic*
June 9, 2010	Ayumi Fujisaki	Atmospheric and Oceanic Science Program, Princeton University, Princeton, New Jersey	*Determinative Factor of Sea-ice Variability in the Sea of Okhotsk Based on a High- resolution Ice-Ocean Coupled Model*
April 29, 2010	Richard Murnane,	Bermuda Institute for Ocean Sciences, St. George, Bermuda	*Some Issues Related to Weather Risk Mitigation: A Panel Discussion*
	Tom Schroeder	UH Meteorology Meteorologist & Entrepreneur	
	Brendan Lane Larson		

IPRC VISITING SCHOLARS

The IPRC has a visiting scholar program. From April 2010 to March 2011, the following scholars visited the IPRC for one week or longer.

NAME	AFFILIATION	DATES
Stephan Lorenz	Max Planck Institute for Meteorology, Hamburg, Germany	4/26/10 – 4/30/10
Richard Murnane	Risk Prediction Initiative, Bermuda Biological Station for Research, St. George, Bermuda	4/27/10 – 4/30/10
Soon-Il An	Yonsei University, Seoul, Korea	7/19/10 – 8/5/10
GaryLagerloef	Earth and Space Research, Seattle, Washington	7/31/10 – 8/4/10
Takatoshi Sakazaki	Hokkaido University, Sapporo, Japan	8/17/10 – 8/26/10
Kazuhiro Oshima	Hokkaido University, Sapporo, Japan	8/23/10 – 10/24/10
Hsin-Chien Liang	National Taiwan Normal University, Taipei, Taiwan	9/1/10 – 9/30/10
Shan Gao	Chinese Academy of Sciences, Beijing, China	9/14/10 – 10/2/10
Hisayuki Kubota	JAMSTEC, RIGC, Yokosuka, Japan	10/5/10 – 12/17/10
Susan Avery	Woods Hole Oceanographic Institution	11/5/10 – 11/12/10
Carsten Eden	University of Hamburg, Hamburg, Germany	11/16/10 – 11/20/10
Tanja Mildner	University of Hamburg, Hamburg, Germany	11/16/10 – 12/15/10
Wataru Ohfuchi	Frontier Research System for Global Change	11/22/10 – 12/10/10
Ming Y. Zhou	National Center for Atmospheric Research, Boulder, Colorado	11/28/10 – 12/11/10
Bunmei Taguchi	JAMSTEC, ESC, Yokohama, Japan	12/6/10 – 3/3/11
Viacheslav Kremenetskiy	Russian Academy of Sciences, Moscow, Russia	1/9/11 – 2/9/11
Sarah Kang	Columbia University, New York, New York	1/14/11 – 1/20/11
In-Sik Kang	Seoul National University, Seoul, Korea	1/14/11 – 2/15/11
Pei-Hsuan Chung	Taipei Municipal University of Education, Taipei, Taiwan	1/17/11 – 2/16/11
Qinyu Liu	Ocean University of China, Qingdao, China	1/20/11 – 2/18/11
Eric Maloney	Colorado State University, Fort Collins, Colorado	1/31/11 – 2/3/11
Yoshio Kawatani	JAMSTEC, ESC, Yokohama, Japan	2/6/11 – 3/8/11
Akio Ishida	JAMSTEC, ESC, Yokohama, Japan	3/2/11 – 3/5/11
Yoshikazu Sasai	JAMSTEC, ESC, Yokohama, Japan	3/3/11 – 3/11/11

IPRC RESEARCH SUPPORT

Institutional Support

Title	PI and Co-PIs	Agency	Amount	Period
JAMSTEC YR 14, (2010 – 2011)	K. Hamilton	JAMSTEC	$2,151,000	04/01/10–03/31/11
Support of Research at the International Pacific Research Center	Not applicable	* University of Hawai'i	$656,679	04/01/10–03/31/11
Data-Intensive Research and Model Development at the International Pacific Research Center	K. Hamilton PI S.P. Xie & P. Hacker	NASA	$5,225,000	03/01/07–02/29/12
Enhancement of Data and Research Activities at the IPRC	K. Hamilton PI P. Hacker & J. Potemra	NOAA / NESDIS	$1,742,160	07/01/09–06/30/10
Enhancement of Data and Research Activities at the IPRC	K. Hamilton PI P. Hacker & J. Potemra	NOAA / NESDIS	$1,489,789	07/01/10–06/30/11

* The University of Hawai'i also provides approximately 16,500 sq. ft. of office space to the IPRC

Individual Grants

Title	PI and Co-PIs	Agency	Amount	Period
Intraseasonal to Decadal Variability and Role of Eddies in the Low-Latitude Western Boundary Current off the Philippines	T. Qu	NSF	$398,318	10/01/10-09/30/13
Early Life Stage Dispersal of Yellowfin Tuna (Thunnus Albacares)	K. Richards	NOAA / PFRP	$121,984	10/01/10-09/30/11
High Resolution Dynamical Projections of Climate Changes for Hawaii and other Pacific Islands	K. Hamilton	US Fish & Wildlife Svc / DOI	$130,026	09/15/10-09/30/13
Pacific Decadal Variability and Central Pacific Warming El Nino in a Changing Climate	N. Schneider	DOE	$132,332	09/15/10-09/14/12
Year 1 – Climate Adaption Partnership for the Pacific (CAPP)	K. Hamilton	E.W. Ctr / NOAA	$182,000	09/01/10-08/31/11
Dynamics of the Boreal Summer Intraseasonal Oscillation: Multi-Scale Interaction	B. Wang, X. Fu, K. Kikuchi	NSF	$597,427	08/15/10-07/31/13
Improved Extended Range Prediction Through a Bayesian Approach: Exploiting the Enhanced Predictability…	S.P. Xie	NOAA	$74,000	08/01/10-07/31/13
Collaborative Research: Mixing in the Equatorial Thermocline (MIXET)	K. Richards, G. Carter, E. Firing, A. Natarov	NSF	$997,185	09/01/10-08/31/14
Climate Change Impacts on Critical Ecosystems in Hawaii and US Pacific Islands Territories	O. Elison Timm, T. Giambelluca	US Fish & Wildlife Svc / DOI	$232,233	09/01/10-09/30/12
Southern Hemisphere Climate and Carbon Cycle Response to Orbital Forcing During the Last ~400,000 Years	A. Timmermann	NSF	$427,199	09/01/10-08/31/13
Interannual Variability of Ocean Vector Winds Near Ocean Fronts and Coastal Orography	S.P. Xie	NASA	$138,673	07/22/10-07/21/14
Dynamics of Near-Surface Eastward Flows in the South Indian Ocean	J. McCreary, R. Furue, J. Potemra	NSF	$446,113	07/01/10-06/30/13

Title	PI and Co-PIs	Agency	Amount	Period
Multi-Model Ensemble Forecasts of Madden-Julian Oscillation	B. Wang & D. Waliser	NOAA / CTB	$734,618	07/01/10-06/30/13
Studies of Predictability of the Intraseasonal Variability Over the East Asian Monsoon System	B. Wang	Busan National University	$42,210	06/28/10-02/28/11
Determining Natural and Anthropogenic Influences on Ocean Acidification Across Micronesia	A. Timmermann	The Nature Conservancy	$30,000	06/08/10-07/31/11
Initialization of Tropical Cyclone Structure for Operational Applications	T. Li	ONR	$45,000	05/01/10-04/30/13
Improvement of APCC Seasonal Prediction and Assessment of Characteristics and Forecast of 2009/2010 Climate Anomalies	B. Wang, J.Y. Lee, J. Fu	APEC Climate Center	$128,221	05/01/10-04/30/11
Estimating Ocean Mixing and Form Drag in the Tropical Pacific	J. McCreary, R. Furue, P. Muller, K. Richards, N. Schneider	NASA	$110,182	02/01/10 – 01/31/12
Sustaining Rice Production in a Changing Climate: Testing Climate Uncertainties and Validating Selected Adaptation Techniques on Farmers Fields	H. Annamalai	Norwegian Embassy	$106,027	01/01/10 – 12/31/12
Basin-Scale Circulation and Mesoscale Dynamics of the Black Sea: Implications for Climate	N. Maximenko A. Zatsepin	US CRDF	$16,000	12/01/09 – 11/30/11
Assessing the Quality of Aquarius Sea Surface Salinity Measurements Using an Ocean State Estimation System	T. Qu	JPL / NASA	$66,093	11/17/09 – 03/31/12
Aquarius Salinity Calibration Error Quantification, Signal-To-Noise Analyses, and Resolution Studies	N. Maximenko, J. Potemra, P. Hacker	NASA	$288,045	10/01/09 – 09/30/13
Improve the Representation of Convection-PBL Interactions in Two Global General Circulation Models (CAM & ECHAM)	X. Fu, B. Wang	DOE	$99,842	09/15/09 – 01/31/11
Collaborative Research: Eddy Dynamics and Impacts of Low-Frequency Variations in the California Current System (supplemental)	N. Schneider	NSF	$189,279	08/19/09 – 02/29/12
Mechanisms and Effects of Tropical Indian Ocean Variability	S.P. Xie	NSF	$525,408	08/15/09 – 07/31/13
Next Generation Aerosol-Cloud Microphysics for Advanced High-Resolution Climate Predictions	K. Hamilton	Univ of Wisconsin / DOE	$292,426	08/15/09 – 08/14/11
Evaluation and Improvements of Cloud and Precipitation Physics in the Operational Hurricane WRF Model at NOAA/EMC	Y. Wang, V. Phillips	NOAA / JHT	$184,547	08/01/09 – 07/31/11
Remote Versus Local Forcing of Intraseasonal Variability in the IAS Region: Consequences for Prediction	S.P. Xie	NOAA / CPPA	$132,174	07/01/09-06/30/12
Collaborative Research: Toward Improved Projections of Abrupt Response to Anthropogenic Forcing: Combining Paleoclimate Proxy and Instrumental Observations with an Earth System Model	A. Timmermann	NSF	$228,675	06/15/09 – 05/31/12
Collaborative Studies on Tropical Cyclone Intensification	T. Li	NPS	$96,144	06/11/09 – 06/10/10
Dynamics of the Descending Branch of the Atlantic Meridional Overturning Circulation	J. McCreary, R. Furue, A. Timmermann	NSF	$443,595	06/01/09-05/31/12
Development of a MME System for ISO Prediction and Improvement of Coupled Model Initialization	B. Wang, J.Y. Lee, Z. Wu	Pusan Nat'l Univ	$124,784	04/22/09 – 04/21/10
A Tropical Cyclone Genesis Forecast Model	T. Li	ONR	$117,300	02/16/09 – 05/31/12
Study of Tropical Cyclone Intensity Change and Genesis with EOS Observations and WRF Model	B. Wang, H. Su, B. Kahn	NASA	$646,197	01/01/09-12/31/12
Dynamics of Anisotropic Mean and Time-Varying Structure of Ocean Circulation	N. Maximenko, E. Di Lorenzo, & N. Schneider	NASA	$534,644	10/01/08 – 09/30/12
Changes of Tropical Pacific Climate Variability During the Last Millennium	A. Timmermann & O. Timm	NOAA	$191,850	07/01/08 – 06/30/13

Title	PI and Co-PIs	Agency	Amount	Period
Development of an Extended and Long-Range Precipitation Prediction System over the Pacific Islands	H. Annamalai	NOAA	$346,086	07/01/08 - 06/30/12
Toward Reducing Climate Model Biases in the Equatorial Atlantic and Adjacent Continents	S.P. Xie & I. Richter	NOAA / CPO	$342,124	07/01/08 – 06/30/11
Precipitation Climatology Projections for Mid and Late 21st Centuries for the Main Hawaiian Islands	K. Hamilton	USGS	$134,854	06/01/08 – 12/31/11
Scale Interactions in the Equatorial Ocean	K. Richards & J. McCreary	NSF	$528,268	05/01/08 – 04/30/12
Study of Processes Leading to Tropical Cyclone Structure and Intensity Changes	Y. Wang	NSF	$398,016	04/01/08 – 03/31/12
Analysis and High-Resolution Modeling of Tropical Cyclogenesis during TCS-08 and TPARC Field Campaign	T. Li & M. Peng	ONR	$212,434	01/01/08 – 12/31/11
Climate Change and Persistent Droughts: Impacts, Vulnerability and Adaptation in Rice Growing Subdivisions of India	H. Annamalai	Norwegian Institute for Agrcltl & Envrmtl Rsch	$115,796	12/07/07– 04/30/11
Collaborative Research: Impacts of Ocean Physics on the Arabian Sea Oxygen Minimum Zone	J. McCreary, K. Richards, & Z. Yu	NSF	$385,570	10/01/07 – 09/30/12
Developing the Hawaii-Pacific Ocean Observing and Information System	J. Potemra, et at.	NOAA	$371,929	10/01/07- 12/31/11
Understanding Annual Cycle-ENSO Interactions in Climate Change Simulations	N. Schneider & A. Timmermann	DOE	$440,724	08/15/07– 08/14/12
Future Projections of Mean and Variability of the Asian Summer Monsoon and Indian Ocean Climate Systems	H. Annamalai	DOE	$701,678	08/01/07– 07/31/12
Evaluation and Improvement of NOAA Climate GCM Air-Sea Interaction Physics: An EPIC/VOCALS Synthesis Project	Y. Wang, S.P. Xie, & S. de Szoeke	NOAA / OGP/CPPA	$275,384	08/01/07 – 07/31/11
Understanding Climate-Biogeochemical Feedbacks During the Last Glacial-Interglacial Transition: A Systematic Modeling and Paleo-Data Synthesis Approach	A. Timmermann	NSF	$314,100	07/01/07– 12/31/10
Collaborative Research: Decadal Coupled Ocean-Atmosphere Interactions in the North	N. Schneider	NSF	$221,682	03/01/07– 02/28/12
Dynamics of the Boreal Summer Intraseasonal Variations	B. Wang & X. Fu	NSF	$526,836	03/01/07– 08/31/10
Western Pacific Tropical Cyclone Reanalysis with the NRL Atmospheric Variational Data Assimilation System (NAVDAS)	T. Li & X. Zhang	ONR	$221,415	01/01/07– 08/31/10
Collaborative Research: Origin, Pathway and Fate of Equatorial 13ºC Water in the Pacific	T. Qu & I. Fukumori	NSF	$486,210	09/01/06– 08/31/10
Orographically Induced Ocean-Atmosphere Interaction: Satellite Observations and Numerical Modeling	S.P. Xie	NASA	$523,839	06/15/06– 12/26/10
Collaborative Research: Eddy Dynamics and Impacts of Low Frequency Variations in the California Current System	N. Schneider	NSF	$193,340	03/01/06– 02/29/12

The University of Hawaiʻi at Mānoa is an equal opportunity/affirmative action institution.